

Charmless Two-body Baryonic B Decays

Chun-Khiang Chua

Department of Physics, National Taiwan University, Taipei, Taiwan 10764, Republic of China

(Dated: May 22, 2019)

We study charmless two-body baryonic B decays in a diagrammatic approach. Relations on decay amplitudes are obtained. In general there are more than one tree and more than one penguin amplitudes. The number of independent amplitudes can be reduced in the large m_B limit. It leads to more predictive results. Some prominent modes for experimental searches are pointed out.

PACS numbers: 11.30.Hv, 13.25.Hw, 14.40.Nd

I. INTRODUCTION

Baryonic modes in B decays are emerging. Decay modes, such as $\bar{B} \rightarrow D^* p \bar{n}$ [1], $D^* p \bar{p}$ [2], $p \bar{p} K^{(*)}$, $p \bar{p} \pi$ [3, 4], $\Lambda \bar{p} \pi^-$ [5] and $\Lambda_c^+ \bar{p}$ [6], have been observed. The $\bar{B}^0 \rightarrow \Lambda_c^+ \bar{p}$ decay having

$$\mathcal{B}(\bar{B}^0 \rightarrow \Lambda_c^+ \bar{p}) = (2.19_{-0.49}^{+0.56} \pm 0.32 \pm 0.57) \times 10^{-5}, \quad (1)$$

is the only two-body mode observed so far [6, 7]. By a simple scaling of $|V_{ub}/V_{cb}|^2$ [8] on the $\bar{B}^0 \rightarrow \Lambda_c^+ \bar{p}$ decay rate, the rates of the charmless modes are expected to be of the order 10^{-7} [6]. This estimation is consistent with the (90% confident level) experimental upper limits [7],

$$\begin{aligned} \mathcal{B}(\bar{B}^0 \rightarrow p \bar{p}) &< 1.2 \times 10^{-6}, \\ \mathcal{B}(\bar{B}^0 \rightarrow \Lambda \bar{\Lambda}) &< 1.0 \times 10^{-6}, \\ \mathcal{B}(B^- \rightarrow \Lambda \bar{p}) &< 2.2 \times 10^{-6}, \end{aligned} \quad (2)$$

obtained by using 31.7 million $B\bar{B}$ events, and is only one order of magnitude below. The number of $B\bar{B}$ samples are accumulating rapidly in B factories. The charmless baryonic modes could be just around the corner.

Motivated by these observations, there are many recent theoretical studies in the three-body decay modes [9–17]. It is pointed out in Ref. [9] that three-body baryonic modes could be enhanced over two-body, by reducing energy release to the baryons via emitting a fast recoil meson. The decay rates of $D^* p \bar{n}$, $D^* p \bar{p}$, $p \bar{p} K$ and $\Lambda \bar{p} \pi^-$ modes can be understood to some extent [10–16] and the spectra, having threshold enhancement behavior, are consistent with predictions [9, 11]. The three-body decays seem to be much involved than the two-body decays. However, in some cases their amplitudes can be related to some well measured quantities, such as nucleon magnetic form factors, under the factorization approximation, and gain better control.

The two-body baryonic decays are in general non-factorizable. One has to resort to model calculations. There are pole model [12, 18–20], sum rule [21], diquark model [22, 23] and flavor symmetry related [24–29] studies. Predictions from various models usually differ a lot and early calculations usually give too large rates. Some technics developed may still be useful. For example, an updated pole model prediction [20] on the $\bar{B}^0 \rightarrow \Lambda_c^+ \bar{p}$ rate is consistent with data [6].

In this work we use a quark diagram (or topological) approach to study charmless two-body baryonic B decays. This approach was developed and applied to the study of the two-body mesonic decays [30–35]. It is closely related to the SU(3) flavor symmetry [30, 33]. Furthermore, it does not rely on any factorization assumption. It is stressed that these topological amplitudes include long-distant and short distant final state interaction (FSI) effects [31, 32]. For example, it is used in the study on FSI in the $\bar{B} \rightarrow DP$ system [35].

Motivated by the recent $\bar{B}^0 \rightarrow \Lambda_c^+ \bar{p}$ observation, the topological approach has been applied to the charmful baryonic case and the FSI effects are studied [29]. We further extend the quark diagram approach to the charmless case and obtain some amplitude relations. In general there are more than one tree and more than one penguin amplitudes. In principle, these amplitudes can be extracted from data. However, so far we do not have any relevant data yet.

It is useful to reduce the number of independent topological amplitudes. We use asymptotic relations [36] to relate various amplitudes. The same technics has been used in the study of the three-body case [12, 14, 15] and it leads to encouraging results. For example, the experiment finding of $\mathcal{B}(\Lambda \bar{p} \pi^-) > \mathcal{B}(\Sigma^0 \bar{p} \pi^-)$ [5] can be understood [15] and tree-body decay spectra are consistent with the QCD counting rule [37] expectations. Due to the large energy release, we expect the asymptotic relations to work better in the two-body case than in the three-body case. For example, the smallness of two-body decay rates may due to some $1/m_B^2$ suppression as expected from QCD counting rules.

The order of this paper is as follows. In Sec. II, we formulate the quark diagram approach for the study of the charmless two-body baryonic B decays. We consider decay modes with decuplet anti-decuplet, octet anti-decuplet, decuplet anti-octet and octet anti-octet baryonic final states. Relations on amplitudes are obtained. In Sec. III, we reduce the number of independent topological amplitudes by considering the large m_B limit. In Sec. IV, we discuss the phenomenology of the charmless two-body baryonic decays. We suggest some prominent modes for experimental searches. In Sec. IV we give discussion and conclusion, followed by an appendix for the derivation of asymptotic relations.

II. TOPOLOGICAL AMPLITUDES OF CHARMLESS $\overline{B} \rightarrow \overline{B}\overline{B}$ DECAYS

In this section we use a quark diagram (or topological) approach to decompose the charmless two-body baryonic decay amplitudes. It is useful to re-derive some familiar results of the mesonic case first. Since quark diagram is a representation of flavor SU(3) symmetry, the topological approach should be closely related to the SU(3) approach [30]. We use the $\overline{B} \rightarrow DP$ decay to illustrate this point and to introduce some useful tools before we turn to the charmless case.

We follow Ref. [38] to decompose $\overline{B} \rightarrow DP$ decay amplitudes according to flavor SU(3) symmetry. We recall that the fields annihilating B^- , $\overline{B}_{d,s}^0$, creating $D^{0,+}$, D_s^+ and creating π , K , η_8 transform respectively as $\overline{\mathbf{3}}$, $\mathbf{3}$ and $\mathbf{8}$ under SU(3) [38, 39],

$$\overline{B} = (B^- \ \overline{B}^0 \ \overline{B}_s^0), \quad \overline{D} = (\overline{D}^0 \ D^- \ D_s^-),$$

$$\Pi = \begin{pmatrix} \frac{\pi^0}{\sqrt{2}} + \frac{\eta_8}{\sqrt{6}} & \pi^+ & K^+ \\ \pi^- & -\frac{\pi^0}{\sqrt{2}} + \frac{\eta_8}{\sqrt{6}} & K^0 \\ K^- & \overline{K}^0 & -\sqrt{\frac{2}{3}}\eta_8 \end{pmatrix}. \quad (3)$$

The $(\bar{d}u)(\bar{c}b)$ operators in the effective Hamiltonian H_W can be expressed as $(\bar{q}_i H_j^i q^j)(\bar{c}b)$, where $q^i = (u, d, s)$ and

$$H = \begin{pmatrix} 0 & 0 & 0 \\ 1 & 0 & 0 \\ 0 & 0 & 0 \end{pmatrix}. \quad (4)$$

The effective Hamiltonian, in term of the meson degree of freedom, for the $\overline{B} \rightarrow DP$ decay should have the same SU(3) transform property of H_W . Consequently, we have [38]

$$H_{\text{eff}} = T \overline{B}_m \overline{D}^m H_j^i \Pi_i^j + C \overline{B}_m \Pi_i^m H_j^i \overline{D}^j + E \overline{B}_i H_j^i \Pi_m^j \overline{D}^m, \quad (5)$$

with probable FSI effects contained in the coefficients. The $\overline{B} \rightarrow DP$ decay amplitudes can be expressed in terms of these coefficients [38]

$$\begin{aligned} A_{D^0\pi^-} &= T + C, & A_{D^+\pi^-} &= T + E, \\ A_{D^0\pi^0} &= \frac{1}{\sqrt{2}}(-C + E), & A_{D_s^+K^-} &= E, \\ A_{D^0\eta_8} &= \frac{1}{\sqrt{6}}(C + E). \end{aligned} \quad (6)$$

The above expression can also be obtained by using the topological approach with the coefficients T , C , E interpreted as the (color-allowed) external W -emission, (color-suppressed) internal W -emission and W -exchange tree amplitudes, respectively [31–35].

The one-to-one correspondence of the SU(3) parameters and the topological amplitudes is not a coincidence.

It can be understood by using a flavor flow analysis. We take the first term of H_{eff} for illustration. In H_W the decays are governed by the $b \rightarrow c \bar{q}^j q_i$ transition with the corresponded H_j^i coupling. The first term of H_{eff} in Eq. (5) is $\overline{B}_m \overline{D}^m H_j^i \Pi_i^j$. The $\overline{B}_m \overline{D}^m$ part can be interpreted as a \overline{B}_m to D^m transition with the same light anti-quark \bar{q}_m (\bar{q}^m)¹ flavor, while the Π_i^j part is responsible for the creation of the meson where the W -emitted $\bar{q}^j q_i$ pair ends up with. The above picture clearly corresponds to the external W -emission topology. Similarly, the identification of the C (E) amplitude to the second (third) term of H_{eff} can be understood in the same way.

It is straightforward to extend the above approach to the charmless case and the well known topological decompositions of the charmless $\overline{B} \rightarrow PP$ decay amplitudes [32–34] can be reproduced. For the $b \rightarrow u\bar{u}d$ and $b \rightarrow q\bar{q}d$ processes, the tree (\mathcal{O}_T) and penguin (\mathcal{O}_P) operators respectively have the following flavor quantum numbers

$$\begin{aligned} \mathcal{O}_T &\sim (b\bar{u})(u\bar{d}) = H_j^{ik}(b\bar{q}_i)(q^j\bar{q}_k), \\ \mathcal{O}_P &\sim (b\bar{q}_i)(q^i\bar{d}) = H^k(b\bar{q}_i)(q^i\bar{q}_k), \end{aligned} \quad (7)$$

with $H_1^{12} = 1 = H^2$, otherwise $H_j^{ik} = H^k = 0$. The flavor structures of $|\Delta S| = 1$ tree and penguin operators can be obtained by replacing d to s and $H_1^{12} = 1 = H^2$ to $H_1^{13} = 1 = H^3$ in the above expression. By using a similar flavor flow analysis as the $\overline{B} \rightarrow DP$ case, we obtain²

$$\begin{aligned} H_{\text{eff}} = & T \overline{B}_m H_j^{ik} \Pi_k^j \Pi_i^m + C \overline{B}_m H_j^{ik} \Pi_i^j \Pi_k^m \\ & + E \overline{B}_k H_j^{ik} \Pi_i^j \Pi_l^l + A \overline{B}_i H_j^{ik} \Pi_l^j \Pi_k^l \\ & + P \overline{B}_m H^k \Pi_i^m \Pi_k^i + \frac{1}{2} PA \overline{B}_k H^k \Pi_m^l \Pi_l^m, \end{aligned} \quad (8)$$

where the A , P and PA terms correspond to annihilation, penguin and penguin annihilation amplitudes, respectively. We can reproduce Table I and II of Ref. [33] (up to some trivial overall sign changes from wave function definitions) by using the above H_{eff} .

We are now ready to turn to the baryonic cases. We will study various decay modes, including decuplet anti-decuplet, decuplet anti-octet, octet anti-decuplet and octet anti-octet baryonic final states. We start from the easiest case, in the sense of flavor structure, and move on with increasing complexity.

A. \overline{B} to decuplet anti-decuplet baryonic decays

It is straightforward to extend the quark diagram approach to the B to decuplet anti-decuplet decay. As

¹ We use subscript and superscript according to the field convention. For example, we assign a subscript (superscript) to the initial (final) state anti-quark \bar{q}_m (\bar{q}^m).

² Note that $H_i^{ik} (= H^k)$ does not lead to any additional term.

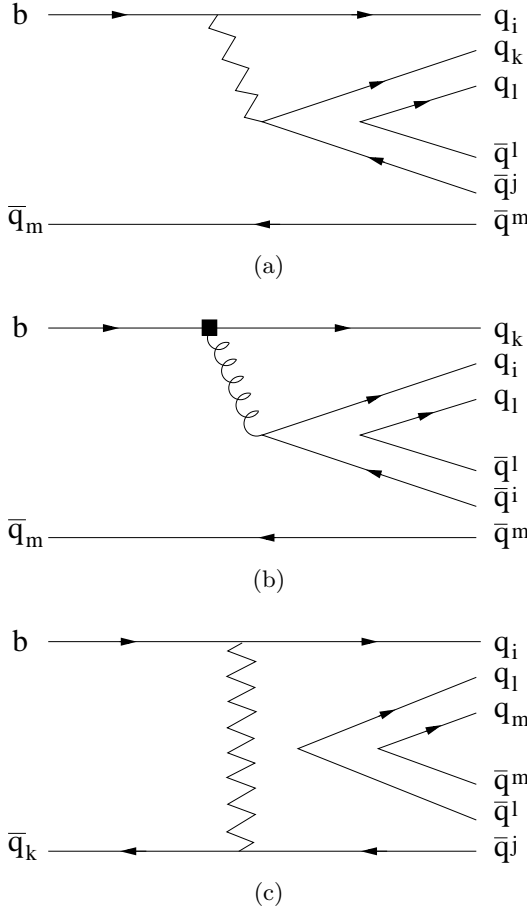


FIG. 1: Pictorial representation of (a) T (tree), (b) P (penguin) and (c) E (W -exchange) amplitudes in \bar{B} to baryon pair decays.

shown in Fig. 1, we have tree (T), penguin (P) and W -exchange (E) amplitudes for processes governed by $\mathcal{O}_{T,P}$. Since there is no external W -exchange diagram and the internal W -exchange amplitude is not color suppressed, we use the symbol T for the tree amplitude.

The decomposition of decay amplitudes can be obtained by using the flavor flow analysis. The first step is to match the flavor. For example, the decuplet with $q_i q_k q_l$ flavor as shown in Fig. 1(a) is produced by the \bar{D}_{ikl} field, while the decuplet with $\bar{q}^l \bar{q}^j \bar{q}^m$ flavor is created by the \mathcal{D}^{jlm} field, where \mathcal{D}^{jlm} is the familiar decuplet field with symmetric flavor indices. To be specified, we use (see, for example [39])

$$\begin{aligned} \mathcal{D}^{111} &= \Delta^{++}, \quad \mathcal{D}^{112} = \frac{1}{\sqrt{3}} \Delta^+, \\ \mathcal{D}^{122} &= \frac{1}{\sqrt{3}} \Delta^0, \quad \mathcal{D}^{222} = \Delta^-, \\ \mathcal{D}^{113} &= \frac{1}{\sqrt{3}} \Sigma^{*+}, \quad \mathcal{D}^{123} = \frac{1}{\sqrt{6}} \Sigma^{*0}, \quad \mathcal{D}^{223} = \frac{1}{\sqrt{3}} \Sigma^{*-}, \\ \mathcal{D}^{133} &= \frac{1}{\sqrt{3}} \Xi^{*0}, \quad \mathcal{D}^{233} = \frac{1}{\sqrt{3}} \Xi^{*-}, \quad \mathcal{D}^{333} = \Omega^-. \end{aligned} \quad (9)$$

Hence by using the flavor flow analysis and the corresponding rule,

$$q_i q_k q_l \rightarrow \bar{D}_{ikl}, \quad \bar{q}^l \bar{q}^j \bar{q}^m \rightarrow \mathcal{D}^{jlm}, \quad (10)$$

we have

$$\begin{aligned} H_{\text{eff}} = & 6 T_{\bar{D}\bar{D}} \bar{B}_m H_j^{ik} \bar{D}_{ikl} \mathcal{D}^{ljm} + 6 P_{\bar{D}\bar{D}} \bar{B}_m H^k \bar{D}_{kil} \mathcal{D}^{lim} \\ & + E_{\bar{D}\bar{D}} \bar{B}_k H_j^{ik} \bar{D}_{ilm} \mathcal{D}^{mlj} + A_{\bar{D}\bar{D}} \bar{B}_i H_j^{ik} \bar{D}_{klm} \mathcal{D}^{mlj} \\ & + PA_{\bar{D}\bar{D}} \bar{B}_k H^k \bar{D}_{lmn} \mathcal{D}^{nml}. \end{aligned} \quad (11)$$

The pre-factors before $T_{\bar{D}\bar{D}}$ and $P_{\bar{D}\bar{D}}$ are assigned for latter purpose. The above equation is an extension of Eq. (8).

It is useful to discuss the QCD counting rules for these amplitudes. In the large m_B limit, we need a hard gluon to create a $q\bar{q}$ pair for the tree or penguin topology. An additional gluon is required to kick the spectator quark in the B meson such that it becomes energetic in the final baryon pair. In the large m_B limit, these amplitudes behave like $\sim 1/m_B^4$. The $1/m_B^4$ factor and the Cabibbo-Kobayashi-Maskawa (CKM) coefficients lead to a suppressed charmless two-body baryonic rates that may be the underlying reason of the negative search result. Other topologies, such as W -exchange ($E_{\bar{D}\bar{D}}$), weak-annihilation $A_{\bar{D}\bar{D}}$ and penguin-annihilation ($PA_{\bar{D}\bar{D}}$) topologies, require an additional $q\bar{q}$ pair creation (see, for example Fig. 1(c)) and are further $1/m_B^2$ suppressed. We should concentrate on T and P amplitudes. The decomposition of \bar{B} to decuplet anti-decuplet decay amplitudes are given in Table I. We use $T^{(\prime)}$ and $P^{(\prime)}$ for the tree and penguin amplitudes, respectively, in $|\Delta S| = 0(1)$ processes.

TABLE I: Decomposition of $\bar{B} \rightarrow \bar{D}\bar{D}$ amplitudes in terms of tree and penguin amplitudes.

Mode	$T_{\bar{D}\bar{D}}$	$P_{\bar{D}\bar{D}}$	Mode	$T'_{\bar{D}\bar{D}}$	$P'_{\bar{D}\bar{D}}$
$B^- \rightarrow \Delta^+ \Delta^{++}$	$2\sqrt{3}$	$2\sqrt{3}$	$B^- \rightarrow \Sigma^{*+} \Delta^{++}$	$2\sqrt{3}$	$2\sqrt{3}$
$\Delta^0 \bar{\Delta}^+$	2	4	$\Sigma^{*0} \bar{\Delta}^+$	$\sqrt{2}$	$2\sqrt{2}$
$\Sigma^{*0} \bar{\Sigma}^{*+}$	$\sqrt{2}$	$2\sqrt{2}$	$\Xi^{*0} \bar{\Sigma}^{*+}$	2	4
$\Sigma^{*-} \bar{\Sigma}^{*0}$	0	$2\sqrt{2}$	$\Xi^{*-} \bar{\Sigma}^{*0}$	0	$2\sqrt{2}$
$\Xi^{*-} \bar{\Xi}^{*0}$	0	2	$\Omega^- \bar{\Xi}^{*0}$	0	$2\sqrt{3}$
$\Delta^- \bar{\Delta}^0$	0	$2\sqrt{3}$	$\Sigma^* \bar{\Delta}^0$	0	2
$\bar{B}^0 \rightarrow \Delta^+ \bar{\Delta}^+$	2	2	$\bar{B}^0 \rightarrow \Sigma^{*+} \bar{\Delta}^+$	2	2
$\Delta^0 \bar{\Delta}^0$	2	4	$\Sigma^{*0} \bar{\Delta}^0$	$\sqrt{2}$	$2\sqrt{2}$
$\Sigma^{*0} \bar{\Sigma}^{*0}$	1	2	$\Xi^{*0} \bar{\Sigma}^{*0}$	$\sqrt{2}$	$2\sqrt{2}$
$\Sigma^{*-} \bar{\Sigma}^{*-}$	0	4	$\Xi^{*-} \bar{\Sigma}^{*-}$	0	4
$\Xi^{*-} \bar{\Xi}^{*-}$	0	2	$\Omega^- \bar{\Xi}^{*-}$	0	$2\sqrt{3}$
$\Delta^- \bar{\Delta}^-$	0	6	$\Sigma^* \bar{\Delta}^-$	0	$2\sqrt{3}$
$\bar{B}_s^0 \rightarrow \Delta^+ \bar{\Sigma}^{*+}$	2	2	$\bar{B}_s^0 \rightarrow \Sigma^{*+} \bar{\Sigma}^{*+}$	2	2
$\Delta^0 \bar{\Sigma}^{*0}$	$\sqrt{2}$	$2\sqrt{2}$	$\Sigma^{*0} \bar{\Sigma}^{*0}$	1	2
$\Sigma^{*0} \bar{\Xi}^{*0}$	$\sqrt{2}$	$2\sqrt{2}$	$\Xi^{*0} \bar{\Xi}^{*0}$	2	4
$\Sigma^{*-} \bar{\Xi}^{*-}$	0	4	$\Xi^{*-} \bar{\Xi}^{*-}$	0	4
$\Xi^{*-} \bar{\Omega}^-$	0	$2\sqrt{3}$	$\Omega^- \bar{\Omega}^-$	0	6
$\Delta^- \bar{\Sigma}^{*-}$	0	$2\sqrt{3}$	$\Sigma^* \bar{\Sigma}^{*-}$	0	2

By using the decay amplitudes shown in Table I we obtain some amplitude relations. For the $\Delta S = 0$ case,

we have

$$\begin{aligned}
A(B^- \rightarrow \Delta^+ \overline{\Delta^{++}}) &= \sqrt{3} A(B^- \rightarrow \Delta^0 \overline{\Delta^+}) + A(B^- \rightarrow \Delta^- \overline{\Delta^0}) = 0, \\
A(B^- \rightarrow \Delta^+ \overline{\Delta^{++}}) &= \sqrt{3} A(\overline{B}^0 \rightarrow \Delta^+ \overline{\Delta^+}) = \sqrt{3} A(\overline{B}_s^0 \rightarrow \Delta^+ \overline{\Sigma^{*+}}), \\
A(B^- \rightarrow \Delta^0 \overline{\Delta^+}) &= A(\overline{B}^0 \rightarrow \Delta^0 \overline{\Delta^0}) = \sqrt{2} A(\overline{B}_s^0 \rightarrow \Delta^0 \overline{\Sigma^{*0}}) \\
&= \sqrt{2} A(B^- \rightarrow \Sigma^{*0} \overline{\Sigma^{*+}}) = 2 A(\overline{B}^0 \rightarrow \Sigma^{*0} \overline{\Sigma^{*0}}) = \sqrt{2} A(\overline{B}_s^0 \rightarrow \Sigma^{*0} \overline{\Xi^{*0}}), \\
2\sqrt{3} A(B^- \rightarrow \Delta^- \overline{\Delta^0}) &= 2 A(\overline{B}^0 \rightarrow \Delta^- \overline{\Delta^-}) = 2\sqrt{3} A(\overline{B}_s^0 \rightarrow \Delta^- \overline{\Sigma^{*-}}) \\
&= 3\sqrt{2} A(B^- \rightarrow \Sigma^{*-} \overline{\Sigma^{*0}}) = 3 A(\overline{B}^0 \rightarrow \Sigma^{*-} \overline{\Sigma^{*0}}) = 3 A(\overline{B}_s^0 \rightarrow \Sigma^{*-} \overline{\Xi^{*0}}) \\
&= 6 A(B^- \rightarrow \Xi^{*-} \overline{\Xi^{*0}}) = 6 A(\overline{B}^0 \rightarrow \Xi^{*-} \overline{\Xi^{*0}}) = 2\sqrt{3} A(\overline{B}_s^0 \rightarrow \Xi^{*-} \overline{\Omega^-}), \tag{12}
\end{aligned}$$

and for the $|\Delta S| = 1$ case, we have

$$\begin{aligned}
A(B^- \rightarrow \Sigma^{*+} \overline{\Delta^{++}}) &= \sqrt{6} A(B^- \rightarrow \Sigma^{*0} \overline{\Delta^+}) + \sqrt{3} A(B^- \rightarrow \Sigma^{*-} \overline{\Delta^0}) = 0, \\
A(B^- \rightarrow \Sigma^{*+} \overline{\Delta^{++}}) &= \sqrt{3} A(\overline{B}^0 \rightarrow \Sigma^{*+} \overline{\Delta^+}) = \sqrt{3} A(\overline{B}_s^0 \rightarrow \Sigma^{*+} \overline{\Sigma^{*+}}), \\
\sqrt{2} A(B^- \rightarrow \Sigma^{*0} \overline{\Delta^+}) &= \sqrt{2} A(\overline{B}^0 \rightarrow \Sigma^{*0} \overline{\Delta^0}) = 2 A(\overline{B}_s^0 \rightarrow \Sigma^{*0} \overline{\Sigma^{*0}}) \\
&= A(B^- \rightarrow \Xi^{*0} \overline{\Sigma^{*+}}) = \sqrt{2} A(\overline{B}^0 \rightarrow \Xi^{*0} \overline{\Sigma^{*0}}) = A(\overline{B}_s^0 \rightarrow \Xi^{*0} \overline{\Xi^{*0}}), \\
6 A(B^- \rightarrow \Sigma^{*-} \overline{\Delta^0}) &= 2\sqrt{3} A(\overline{B}^0 \rightarrow \Sigma^{*-} \overline{\Delta^-}) = 6 A(\overline{B}_s^0 \rightarrow \Sigma^{*-} \overline{\Sigma^{*-}}) \\
&= 3\sqrt{2} A(B^- \rightarrow \Xi^{*-} \overline{\Sigma^{*0}}) = 3 A(\overline{B}^0 \rightarrow \Xi^{*-} \overline{\Sigma^{*0}}) = 3 A(\overline{B}_s^0 \rightarrow \Xi^{*-} \overline{\Xi^{*0}}) \\
&= 2\sqrt{3} A(B^- \rightarrow \Omega^- \overline{\Xi^{*0}}) = 2\sqrt{3} A(\overline{B}^0 \rightarrow \Omega^- \overline{\Xi^{*0}}) = 2 A(\overline{B}_s^0 \rightarrow \Omega^- \overline{\Omega^-}). \tag{13}
\end{aligned}$$

These relations are consistent with Ref. [28]. Note that some results in Ref. [28] are obtained by considering dominant tree or penguin amplitudes only, while the above relations include both contributions.

B. \overline{B} to decuplet anti-octet, octet anti-decuplet baryonic decays

We extend the previous case to the $\overline{B} \rightarrow \mathcal{B}\overline{D}$, $\mathcal{D}\overline{B}$ cases. Note that the (anti-)decuplet parts are as before. For the octet part, we use [39]

$$\mathcal{B} = \begin{pmatrix} \frac{\Sigma^0}{\sqrt{2}} + \frac{\Lambda}{\sqrt{6}} & \Sigma^+ & p \\ \Sigma^- & -\frac{\Sigma^0}{\sqrt{2}} + \frac{\Lambda}{\sqrt{6}} & n \\ \Xi^- & \Xi^0 & -\sqrt{\frac{2}{3}}\Lambda \end{pmatrix}. \tag{14}$$

The \mathcal{B}_k^j has a flavor structure $q^j q^a q^b \epsilon_{abk} - \frac{1}{3} \delta_k^j q^c q^a q^b$ [39]. To match the $q_i q_k q_l$, $\bar{q}^l \bar{q}^j \bar{q}^m$ flavor contents of final state octet baryons (as shown in Fig. 1), we use

$$\begin{aligned}
q_i q_k q_l &\rightarrow \epsilon_{ika} \overline{\mathcal{B}}_l^a, \quad \epsilon_{ial} \overline{\mathcal{B}}_k^a, \quad \epsilon_{akl} \overline{\mathcal{B}}_i^a, \\
\bar{q}^l \bar{q}^j \bar{q}^m &\rightarrow \epsilon^{ljb} \mathcal{B}_b^m, \quad \epsilon^{lbn} \mathcal{B}_b^j, \quad \epsilon^{bjm} \mathcal{B}_b^l, \tag{15}
\end{aligned}$$

as the corresponding fields in H_{eff} . In fact, not all terms in the above equation are independent. They are con-

strained by

$$\epsilon_{ika} \overline{\mathcal{B}}_l^a + \epsilon_{ial} \overline{\mathcal{B}}_k^a + \epsilon_{akl} \overline{\mathcal{B}}_i^a = 0 = \epsilon^{ljb} \mathcal{B}_b^m + \epsilon^{lbn} \mathcal{B}_b^j + \epsilon^{bjm} \mathcal{B}_b^l, \tag{16}$$

which can be shown easily. Hence for each of the $q_i q_k q_l$ and $\bar{q}^l \bar{q}^j \bar{q}^m$ configuration we only need two independent terms.

We are now ready to obtain the effective Hamiltonian for the $B \rightarrow \mathcal{B}\overline{D}$ decays. By replacing $\overline{\mathcal{D}}_{ikl}$ in Eq. (11) by $\epsilon_{ika} \overline{\mathcal{B}}_l^a$ and $\epsilon_{akl} \overline{\mathcal{B}}_i^a$, we have

$$\begin{aligned}
H_{\text{eff}} &= -\sqrt{6} T_{1\mathcal{B}\overline{D}} \overline{B}_m H_j^{ik} \epsilon_{ika} \overline{\mathcal{B}}_l^a \mathcal{D}^{ljm} \\
&\quad -\sqrt{6} T_{2\mathcal{B}\overline{D}} \overline{B}_m H_j^{ik} \epsilon_{akl} \overline{\mathcal{B}}_i^a \mathcal{D}^{ljm} \\
&\quad -\sqrt{6} P_{\mathcal{B}\overline{D}} \overline{B}_m H^k \epsilon_{kia} \overline{\mathcal{B}}_l^a \mathcal{D}^{lim}, \tag{17}
\end{aligned}$$

where some pre-factors are introduced for later purpose. As argued previously, we shall concentrate on T and P terms. Note that we have two tree and one penguin amplitudes. We use T' and P' for the $|\Delta S| = 1$ case. The resulting decompositions are shown in Table II.

There are relations on decay amplitudes. By using Table II, we have

TABLE II: Decomposition of $\bar{B} \rightarrow \mathcal{B}\bar{\mathcal{D}}$ amplitudes in terms of tree and penguin amplitudes.

Mode	$T_{1\mathcal{B}\bar{\mathcal{D}}}$	$T_{2\mathcal{B}\bar{\mathcal{D}}}$	$P_{\mathcal{B}\bar{\mathcal{D}}}$	Mode	$T'_{1\mathcal{B}\bar{\mathcal{D}}}$	$T'_{2\mathcal{B}\bar{\mathcal{D}}}$	$P'_{\mathcal{B}\bar{\mathcal{D}}}$
$B^- \rightarrow p\bar{\Delta}^{++}$	$-\sqrt{6}$	$\sqrt{6}$	$\sqrt{6}$	$B^- \rightarrow \Sigma^+\bar{\Delta}^{++}$	$\sqrt{6}$	$-\sqrt{6}$	$-\sqrt{6}$
$n\bar{\Delta}^+$	$-\sqrt{2}$	0	$\sqrt{2}$	$\Xi^0\bar{\Sigma}^{*+}$	$\sqrt{2}$	0	$-\sqrt{2}$
$\Lambda\bar{\Sigma}^{*+}$	$2/\sqrt{3}$	$-1/\sqrt{3}$	$-\sqrt{3}$	$\Lambda\bar{\Delta}^+$	$1/\sqrt{3}$	$1/\sqrt{3}$	0
$\Sigma^0\bar{\Sigma}^{*+}$	0	-1	-1	$\Sigma^0\bar{\Delta}^+$	-1	1	2
$\Sigma^-\bar{\Sigma}^{*0}$	0	0	-1	$\Sigma^-\bar{\Delta}^0$	0	0	$\sqrt{2}$
$\Xi^-\bar{\Xi}^{*0}$	0	0	$-\sqrt{2}$	$\Xi^-\bar{\Sigma}^{*0}$	0	0	1
$\bar{B}^0 \rightarrow p\bar{\Delta}^+$	$-\sqrt{2}$	$\sqrt{2}$	$\sqrt{2}$	$\bar{B}^0 \rightarrow \Sigma^+\bar{\Delta}^+$	$\sqrt{2}$	$-\sqrt{2}$	$-\sqrt{2}$
$n\bar{\Delta}^0$	$-\sqrt{2}$	0	$\sqrt{2}$	$\Xi^0\bar{\Sigma}^{*0}$	1	0	-1
$\Lambda\bar{\Sigma}^{*0}$	$\sqrt{2}/3$	$-1/\sqrt{6}$	$-\sqrt{3}/2$	$\Lambda\bar{\Delta}^0$	$1/\sqrt{3}$	$1/\sqrt{3}$	0
$\Sigma^0\bar{\Sigma}^{*0}$	0	$-1/\sqrt{2}$	$-1/\sqrt{2}$	$\Sigma^0\bar{\Delta}^0$	-1	1	2
$\Sigma^-\bar{\Sigma}^{*-}$	0	0	$-\sqrt{2}$	$\Sigma^-\bar{\Delta}^-$	0	0	$\sqrt{6}$
$\Xi^-\bar{\Xi}^{*-}$	0	0	$-\sqrt{2}$	$\Xi^-\bar{\Sigma}^{*-}$	0	0	$\sqrt{2}$
$\bar{B}_s^0 \rightarrow p\bar{\Sigma}^{*+}$	$-\sqrt{2}$	$\sqrt{2}$	$\sqrt{2}$	$\bar{B}_s^0 \rightarrow \Sigma^+\bar{\Sigma}^{*+}$	$\sqrt{2}$	$-\sqrt{2}$	$-\sqrt{2}$
$n\bar{\Sigma}^{*0}$	-1	0	1	$\Xi^0\bar{\Xi}^{*0}$	$\sqrt{2}$	0	$-\sqrt{2}$
$\Lambda\bar{\Xi}^{*0}$	$2/\sqrt{3}$	$-1/\sqrt{3}$	$-\sqrt{3}$	$\Lambda\bar{\Sigma}^{*0}$	$1/\sqrt{6}$	$1/\sqrt{6}$	0
$\Sigma^0\bar{\Xi}^{*0}$	0	-1	-1	$\Sigma^0\bar{\Sigma}^{*0}$	$-1/\sqrt{2}$	$1/\sqrt{2}$	$\sqrt{2}$
$\Sigma^-\bar{\Xi}^{*-}$	0	0	$-\sqrt{2}$	$\Sigma^-\bar{\Sigma}^{*-}$	0	0	$\sqrt{2}$
$\Xi^-\bar{\Omega}^-$	0	0	$-\sqrt{6}$	$\Xi^-\bar{\Xi}^{*-}$	0	0	$\sqrt{2}$

TABLE III: Decomposition of $\bar{B} \rightarrow \mathcal{D}\bar{\mathcal{B}}$ amplitudes in terms of tree and penguin amplitudes.

Mode	$T_{1\mathcal{D}\bar{\mathcal{B}}}$	$T_{2\mathcal{D}\bar{\mathcal{B}}}$	$P_{\mathcal{D}\bar{\mathcal{B}}}$	Mode	$T'_{1\mathcal{D}\bar{\mathcal{B}}}$	$T'_{2\mathcal{D}\bar{\mathcal{B}}}$	$P'_{\mathcal{D}\bar{\mathcal{B}}}$
$B^- \rightarrow \Delta^0\bar{p}$	$\sqrt{2}$	0	$-\sqrt{2}$	$B^- \rightarrow \Sigma^{*0}\bar{p}$	1	0	-1
$\Sigma^{*0}\bar{\Sigma}^+$	-1	0	1	$\Xi^{*0}\bar{\Sigma}^+$	$-\sqrt{2}$	0	$\sqrt{2}$
$\Sigma^{*-}\bar{\Lambda}$	0	0	$\sqrt{3}$	$\Xi^{*-}\bar{\Lambda}$	0	0	$\sqrt{3}$
$\Sigma^{*-}\bar{\Sigma}^0$	0	0	-1	$\Xi^{*-}\bar{\Sigma}^0$	0	0	-1
$\Xi^{*-}\bar{\Xi}^0$	0	0	$\sqrt{2}$	$\Omega^-\bar{\Xi}^0$	0	0	$\sqrt{6}$
$\Delta^-\bar{n}$	0	0	$-\sqrt{6}$	$\Sigma^{*-}\bar{n}$	0	0	$-\sqrt{2}$
$\bar{B}^0 \rightarrow \Sigma^{*0}\bar{\Sigma}^0$	$1/\sqrt{2}$	0	$-1/\sqrt{2}$	$\bar{B}^0 \rightarrow \Xi^{*0}\bar{\Sigma}^0$	1	0	-1
$\Delta^0\bar{n}$	$\sqrt{2}$	$-\sqrt{2}$	$\sqrt{2}$	$\Sigma^{*0}\bar{n}$	1	-1	1
$\Sigma^{*0}\bar{\Lambda}$	$-1/\sqrt{6}$	$\sqrt{2}/3$	$-\sqrt{3}/2$	$\Xi^{*0}\bar{\Lambda}$	$-1/\sqrt{3}$	$2/\sqrt{3}$	$-\sqrt{3}$
$\Delta^+\bar{p}$	0	$-\sqrt{2}$	$\sqrt{2}$	$\Sigma^{*+}\bar{p}$	0	$-\sqrt{2}$	$\sqrt{2}$
$\Sigma^{*-}\bar{\Sigma}^-$	0	0	$-\sqrt{2}$	$\Xi^{*-}\bar{\Sigma}^-$	0	0	$-\sqrt{2}$
$\Xi^{*-}\bar{\Xi}^-$	0	0	$-\sqrt{2}$	$\Omega^-\bar{\Xi}^-$	0	0	$-\sqrt{6}$
$\bar{B}_s^0 \rightarrow \Sigma^{*0}\bar{\Xi}^0$	-1	1	-1	$\bar{B}_s^0 \rightarrow \Xi^{*0}\bar{\Xi}^0$	$-\sqrt{2}$	$\sqrt{2}$	$-\sqrt{2}$
$\Delta^0\bar{\Lambda}$	$-2/\sqrt{3}$	$1/\sqrt{3}$	0	$\Sigma^{*0}\bar{\Lambda}$	$-\sqrt{2}/3$	$1/\sqrt{6}$	0
$\Delta^0\bar{\Sigma}^0$	0	-1	2	$\Sigma^{*0}\bar{\Sigma}^0$	0	$-1/\sqrt{2}$	$\sqrt{2}$
$\Delta^+\bar{\Sigma}^+$	0	$\sqrt{2}$	$-\sqrt{2}$	$\Sigma^{*+}\bar{\Sigma}^+$	0	$\sqrt{2}$	$-\sqrt{2}$
$\Sigma^{*-}\bar{\Xi}^-$	0	0	$\sqrt{2}$	$\Xi^{*-}\bar{\Xi}^-$	0	0	$\sqrt{2}$
$\Delta^-\bar{\Sigma}^-$	0	0	$\sqrt{6}$	$\Sigma^{*-}\bar{\Sigma}^-$	0	0	$\sqrt{2}$

$$\begin{aligned}
& \sqrt{2} A(B^- \rightarrow n\bar{\Delta}^+) + \sqrt{3} A(B^- \rightarrow \Lambda\bar{\Sigma}^{*+}) - A(B^- \rightarrow \Sigma^0\bar{\Sigma}^{*+}) = 0, \\
& A(B^- \rightarrow p\bar{\Delta}^{++}) + \sqrt{3} A(B^- \rightarrow n\bar{\Delta}^+) + 3\sqrt{2} A(B^- \rightarrow \Lambda\bar{\Sigma}^{*+}) - \sqrt{6} A(B^- \rightarrow \Sigma^-\bar{\Sigma}^{*0}) = 0, \\
& A(B^- \rightarrow p\bar{\Delta}^{++}) = \sqrt{3} A(\bar{B}^0 \rightarrow p\bar{\Delta}^+) = \sqrt{3} A(\bar{B}_s^0 \rightarrow p\bar{\Sigma}^{*+}), \\
& A(B^- \rightarrow n\bar{\Delta}^+) = A(\bar{B}^0 \rightarrow n\bar{\Delta}^0) = \sqrt{2} A(\bar{B}_s^0 \rightarrow n\bar{\Sigma}^{*+}), \\
& A(B^- \rightarrow \Lambda(\Sigma^0)\bar{\Sigma}^{*+}) = \sqrt{2} A(\bar{B}^0 \rightarrow \Lambda(\Sigma^0)\bar{\Sigma}^{*0}) = A(\bar{B}_s^0 \rightarrow \Lambda(\Sigma^0)\bar{\Xi}^{*0}), \\
& \sqrt{6} A(B^- \rightarrow \Sigma^-\bar{\Sigma}^{*0}) = \sqrt{3} A(\bar{B}^0 \rightarrow \Sigma^-\bar{\Sigma}^{*-}) = \sqrt{3} A(\bar{B}_s^0 \rightarrow \Sigma^-\bar{\Xi}^{*-}) \\
& = \sqrt{3} A(B^- \rightarrow \Xi^-\bar{\Xi}^{*0}) = \sqrt{3} A(\bar{B}^0 \rightarrow \Xi^-\bar{\Xi}^{*-}) = A(\bar{B}_s^0 \rightarrow \Xi^-\bar{\Omega}^-), \tag{18}
\end{aligned}$$

for the $\Delta S = 0$ case and

$$\begin{aligned}
\sqrt{2} A(B^- \rightarrow \Xi^0 \bar{\Sigma}^{*+}) &- \sqrt{3} A(B^- \rightarrow \Lambda \bar{\Delta}^+) + A(B^- \rightarrow \Sigma^0 \bar{\Delta}^+) = 0, \\
A(B^- \rightarrow \Sigma^+ \bar{\Delta}^{++}) &- 2\sqrt{3} A(B^- \rightarrow \Xi^0 \bar{\Sigma}^{*+}) + 3\sqrt{2} A(B^- \rightarrow \Lambda \bar{\Delta}^+) - \sqrt{3} A(B^- \rightarrow \Sigma^- \bar{\Delta}^0) = 0, \\
A(B^- \rightarrow \Sigma^+ \bar{\Delta}^{++}) &= \sqrt{3} A(\bar{B}^0 \rightarrow \Sigma^+ \bar{\Delta}^+) = \sqrt{3} A(\bar{B}_s^0 \rightarrow \Sigma^+ \bar{\Sigma}^{*+}), \\
A(B^- \rightarrow \Xi^0 \bar{\Sigma}^{*+}) &= \sqrt{2} A(\bar{B}^0 \rightarrow \Xi^0 \bar{\Sigma}^{*0}) = A(\bar{B}_s^0 \rightarrow \Xi^0 \bar{\Xi}^{*0}), \\
A(B^- \rightarrow \Lambda(\Sigma^0) \bar{\Delta}^+) &= A(\bar{B}^0 \rightarrow \Lambda(\Sigma^0) \bar{\Delta}^0) = \sqrt{2} A(\bar{B}_s^0 \rightarrow \Lambda(\Sigma^0) \bar{\Sigma}^{*0}), \\
\sqrt{3} A(B^- \rightarrow \Sigma^- \bar{\Delta}^0) &= A(\bar{B}^0 \rightarrow \Sigma^- \bar{\Delta}^-) = \sqrt{3} A(\bar{B}_s^0 \rightarrow \Sigma^- \bar{\Sigma}^{*-}) \\
&= \sqrt{6} A(B^- \rightarrow \Xi^- \bar{\Sigma}^{*0}) = \sqrt{3} A(\bar{B}^0 \rightarrow \Xi^- \bar{\Sigma}^{*-}) = \sqrt{3} A(\bar{B}_s^0 \rightarrow \Xi^- \bar{\Xi}^{*-}), \tag{19}
\end{aligned}$$

for the $|\Delta S| = 1$ case.

In Table II we find that the penguin-dominated ($|\Delta S| = 1$) $\bar{B} \rightarrow \Lambda \bar{\Delta}$ decays do not receive any penguin contribution. This can be easily understood. In the penguin topology, the s quark of Λ is from the $b \rightarrow s$ decay, so the u, d quarks of Λ are correlated to their pair-creating partners, the \bar{u}, \bar{d} anti-quarks, in the accompanying anti-decuplet baryon. The anti-symmetry property of the Λ wave function and the symmetry property of the anti-decuplet wave function are responsible for the vanishing of the corresponding penguin amplitudes.

We now turn to the $B \rightarrow \mathcal{D} \bar{B}$ case. By replacing \mathcal{D}^{ljm} in Eq. (11) by $\epsilon^{ljb} \mathcal{B}_b^m$ and $\epsilon^{bjm} \mathcal{B}_b^l$ for the decays, we have

$$\begin{aligned}
H_{\text{eff}} = & -\sqrt{6} T_{1\mathcal{D}\bar{B}} \bar{B}_m H_j^{ik} \bar{\mathcal{D}}_{ikl} \epsilon^{ljb} \mathcal{B}_b^m \\
& -\sqrt{6} T_{2\mathcal{D}\bar{B}} \bar{B}_m H_j^{ik} \bar{\mathcal{D}}_{ikl} \epsilon^{bjm} \mathcal{B}_b^l \\
& +\sqrt{6} P_{\mathcal{D}\bar{B}} \bar{B}_m H^k \bar{\mathcal{D}}_{kil} \epsilon^{bim} \mathcal{B}_b^l. \tag{20}
\end{aligned}$$

We have two tree and one penguin amplitudes.

The decomposition of decay amplitudes are shown in Table III. From the table, we have

$$\begin{aligned}
\sqrt{3} A(B^- \rightarrow \Delta^0 \bar{p}) + \sqrt{3} A(\bar{B}^0 \rightarrow \Delta^+ \bar{p}) &= A(B^- \rightarrow \Delta^- \bar{n}) + \sqrt{3} A(\bar{B}^0 \rightarrow \Delta^0 \bar{n}), \\
A(B^- \rightarrow \Delta^0 \bar{p}) &= -\sqrt{2} A(B^- \rightarrow \Sigma^{*0} \bar{\Sigma}^+) = 2 A(\bar{B}^0 \rightarrow \Sigma^{*0} \bar{\Sigma}^0), \\
A(\bar{B}^0 \rightarrow \Delta^0 \bar{n}) &= -\sqrt{2} A(\bar{B}_s^0 \rightarrow \Sigma^{*0} \bar{\Xi}^0), \\
A(\bar{B}^0 \rightarrow \Delta^+ \bar{p}) &= -A(\bar{B}_s^0 \rightarrow \Delta^+ \bar{\Sigma}^+), \\
A(B^- \rightarrow \Delta^- \bar{n}) &= -\sqrt{2} A(B^- \rightarrow \Sigma^{*-} \bar{\Lambda}) = \sqrt{6} A(B^- \rightarrow \Sigma^{*-} \bar{\Sigma}^0) \\
&= -\sqrt{3} A(B^- \rightarrow \Xi^{*-} \bar{\Xi}^0) = \sqrt{3} A(\bar{B}^0 \rightarrow \Xi^{*-} \bar{\Xi}^-) = \sqrt{3} A(\bar{B}^0 \rightarrow \Sigma^{*-} \bar{\Sigma}^-) \\
&= -\sqrt{3} A(\bar{B}_s^0 \rightarrow \Sigma^{*-} \bar{\Xi}^-) = -A(\bar{B}_s^0 \rightarrow \Delta^- \bar{\Sigma}^-), \tag{21}
\end{aligned}$$

for $\Delta S = 0$ processes, and

$$\begin{aligned}
\sqrt{2} A(B^- \rightarrow \Sigma^{*0} \bar{p}) + A(\bar{B}^0 \rightarrow \Sigma^{*+} \bar{p}) &= A(B^- \rightarrow \Sigma^{*-} \bar{n}) + \sqrt{2} A(\bar{B}^0 \rightarrow \Sigma^{*0} \bar{n}), \\
\sqrt{2} A(B^- \rightarrow \Sigma^{*0} \bar{p}) &= -A(B^- \rightarrow \Xi^{*0} \bar{\Sigma}^+) = \sqrt{2} A(\bar{B}^0 \rightarrow \Xi^{*0} \bar{\Sigma}^0), \\
\sqrt{2} A(\bar{B}^0 \rightarrow \Sigma^{*0} \bar{n}) &= -A(\bar{B}_s^0 \rightarrow \Xi^{*0} \bar{\Xi}^0), \\
A(\bar{B}^0 \rightarrow \Sigma^{*+} \bar{p}) &= -A(\bar{B}_s^0 \rightarrow \Sigma^{*+} \bar{\Sigma}^+), \\
\sqrt{3} A(B^- \rightarrow \Sigma^{*-} \bar{n}) &= -A(B^- \rightarrow \Omega^- \bar{\Xi}^0) = A(\bar{B}^0 \rightarrow \Omega^- \bar{\Xi}^-) \\
&= -\sqrt{2} A(B^- \rightarrow \Xi^{*-} \bar{\Lambda}) = \sqrt{6} A(B^- \rightarrow \Xi^{*-} \bar{\Sigma}^0) = \sqrt{3} A(\bar{B}^0 \rightarrow \Xi^{*-} \bar{\Sigma}^-) \\
&= -\sqrt{3} A(\bar{B}_s^0 \rightarrow \Xi^{*-} \bar{\Xi}^-) = -\sqrt{3} A(\bar{B}_s^0 \rightarrow \Sigma^{*-} \bar{\Sigma}^-), \tag{22}
\end{aligned}$$

for $|\Delta S| = 1$ processes. The implication of Table II and Table III on the phenomenology of the corresponding decay modes will be discussed later.

C. \bar{B} to octet anti-octet baryonic decays

The decomposition of $\bar{B} \rightarrow \mathcal{B} \bar{B}$ amplitudes can be achieved similarly. To obtain the corresponding decay

TABLE IV: Decomposition of $\overline{B} \rightarrow \mathcal{B}\overline{\mathcal{B}}$ amplitudes for $\Delta S = 0$ transitions in terms of tree and penguin amplitudes.

Mode	$T_{1\mathcal{B}\overline{\mathcal{B}}}$	$T_{2\mathcal{B}\overline{\mathcal{B}}}$	$T_{3\mathcal{B}\overline{\mathcal{B}}}$	$T_{4\mathcal{B}\overline{\mathcal{B}}}$	$P_{1\mathcal{B}\overline{\mathcal{B}}}$	$P_{2\mathcal{B}\overline{\mathcal{B}}}$
$B^- \rightarrow n\overline{p}$	-1	0	0	0	-5	0
$\Lambda\overline{\Sigma}^+$	$-\sqrt{2/3}$	0	$1/\sqrt{6}$	0	$-5/\sqrt{6}$	$-5/\sqrt{6}$
$\Sigma^-\overline{\Lambda}$	0	0	0	0	$-5/\sqrt{6}$	$-5/\sqrt{6}$
$\Sigma^-\overline{\Sigma^0}$	0	0	0	0	$-5/\sqrt{2}$	$5/\sqrt{2}$
$\Sigma^0\overline{\Sigma^+}$	0	0	$1/\sqrt{2}$	0	$5/\sqrt{2}$	$-5/\sqrt{2}$
$\Xi^-\overline{\Xi^0}$	0	0	0	0	0	-5
$B^0 \rightarrow p\overline{p}$	0	1	0	-1	0	5
$n\overline{n}$	-1	1	0	0	-5	5
$\Lambda\overline{\Lambda}$	$-1/3$	$2/3$	$1/6$	$-1/3$	$-5/6$	$25/6$
$\Lambda\overline{\Sigma^0}$	$1/\sqrt{3}$	0	$-1/2\sqrt{3}$	0	$5/2\sqrt{3}$	$5/2\sqrt{3}$
$\Sigma^0\overline{\Lambda}$	0	0	$1/2\sqrt{3}$	$-1/\sqrt{3}$	$5/2\sqrt{3}$	$5/2\sqrt{3}$
$\Sigma^-\overline{\Sigma^-}$	0	0	0	0	-5	5
$\Sigma^0\overline{\Sigma^0}$	0	0	-1/2	0	-5/2	$5/2$
$\Xi^-\overline{\Xi^-}$	0	0	0	0	0	5
$B_s^0 \rightarrow p\overline{\Sigma^+}$	0	-1	0	1	0	-5
$n\overline{\Lambda}$	$\sqrt{2/3}$	$-1/\sqrt{6}$	0	0	$10/\sqrt{6}$	$-5/\sqrt{6}$
$n\overline{\Sigma^0}$	0	$1/\sqrt{2}$	0	0	0	$5/\sqrt{2}$
$\Lambda\overline{\Xi^0}$	$-\sqrt{2/3}$	$\sqrt{2/3}$	$1/\sqrt{6}$	$-1/\sqrt{6}$	$-5/\sqrt{6}$	$10/\sqrt{6}$
$\Sigma^0\overline{\Xi^0}$	0	0	$1/\sqrt{2}$	$-1/\sqrt{2}$	$5/\sqrt{2}$	0
$\Sigma^-\overline{\Xi^-}$	0	0	0	0	-5	0

effective Hamiltonian, we replace $\overline{\mathcal{D}}_{ikl}$ (\mathcal{D}^{ljm}) in Eq. (11) by $\epsilon_{ika}\overline{\mathcal{B}}_l^a$ and $\epsilon_{akl}\overline{\mathcal{B}}_i^a$ ($\epsilon^{ljb}\mathcal{B}_b^m$ and $\epsilon^{bjm}\mathcal{B}_b^l$). We have

$$\begin{aligned}
H_{\text{eff}} = & T_{1\mathcal{B}\overline{\mathcal{B}}} \overline{B}_m H_j^{ik} \epsilon_{ika} \overline{\mathcal{B}}_l^a \epsilon^{ljb} \mathcal{B}_b^m \\
& + T_{2\mathcal{B}\overline{\mathcal{B}}} \overline{B}_m H_j^{ik} \epsilon_{ika} \overline{\mathcal{B}}_l^a \epsilon^{bjm} \mathcal{B}_b^l \\
& + T_{3\mathcal{B}\overline{\mathcal{B}}} \overline{B}_m H_j^{ik} \epsilon_{akl} \overline{\mathcal{B}}_i^a \epsilon^{ljb} \mathcal{B}_b^m \\
& + T_{4\mathcal{B}\overline{\mathcal{B}}} \overline{B}_m H_j^{ik} \epsilon_{akl} \overline{\mathcal{B}}_i^a \epsilon^{bjm} \mathcal{B}_b^l \\
& - 5 P_{1\mathcal{B}\overline{\mathcal{B}}} \overline{B}_m H^k \epsilon_{kia} \overline{\mathcal{B}}_l^a \epsilon^{lib} \mathcal{B}_b^m \\
& - 5 P_{2\mathcal{B}\overline{\mathcal{B}}} \overline{B}_m H^k \epsilon_{kia} \overline{\mathcal{B}}_l^a \epsilon^{bim} \mathcal{B}_b^l. \quad (23)
\end{aligned}$$

The coefficients are assigned for later purpose.

There are four tree amplitudes and two penguin amplitudes. For the tree amplitudes all four combinations as suggested in Eqs. (15, 16) are used. For the penguin part, only two of the four combinations are independent. The two combinations used in the penguin amplitudes can be expressed as

$$\begin{aligned}
\epsilon_{kia} \overline{\mathcal{B}}_l^a \epsilon^{lib} \mathcal{B}_b^m &= \frac{1}{2} \{ \mathcal{B}, \overline{\mathcal{B}} \}_k^m + \frac{1}{2} [\mathcal{B}, \overline{\mathcal{B}}]_k^m, \\
\epsilon_{kia} \overline{\mathcal{B}}_l^a \epsilon^{bim} \mathcal{B}_b^l &= \frac{1}{2} \{ \mathcal{B}, \overline{\mathcal{B}} \}_k^m - \frac{1}{2} [\mathcal{B}, \overline{\mathcal{B}}]_k^m - \delta_k^m \text{Tr}(\mathcal{B}\overline{\mathcal{B}}). \quad (24)
\end{aligned}$$

One can readily recognize the anti-commutator and the commutator parts as D and F -terms in the usual SU(3) combination when dealing with an operator having $\bar{q}_k H_m^k q^m$ flavor quantum number [39]. The $\text{Tr}(\mathcal{B}\overline{\mathcal{B}})$ term, as denoted as S in Ref. [14], is needed in a non-traceless H_m^k case. If we use the D - F - S basis instead of

the $\epsilon \overline{\mathcal{B}} \epsilon \mathcal{B}$ basis, we will have

$$P_D = \frac{1}{2}(P_1 + P_2), \quad P_F = \frac{1}{2}(P_1 - P_2), \quad P_S = -P_2. \quad (25)$$

Since we only have two independent components, we have a constraint: $P_D - P_F + P_S = 0$. This is nothing but the Okubo-Zweig-Iizuka (OZI) rule in the $\mathcal{B}\overline{\mathcal{B}}$ sector. A similar constraint is used in Ref. [14], where it is enforced by handed. The OZI rule is satisfied automatically in this approach, since we are matching the baryon quark flavors (see, Fig. 1) in the beginning.

We shown in Table IV (V) the decay amplitudes for $|\Delta S| = 0$ (1) processes. From the tables, we obtain

$$\begin{aligned}
\sqrt{3} A(B^- \rightarrow \Lambda\overline{\Sigma}^+) &= A(B^- \rightarrow \Sigma^0\overline{\Sigma}^+) \\
&+ \sqrt{2} A(B^- \rightarrow n\overline{p}), \\
\sqrt{3} A(B^- \rightarrow \Sigma^-\overline{\Lambda}) &= A(B^- \rightarrow \Sigma^-\overline{\Sigma^0}) \\
&+ \sqrt{2} A(B^- \rightarrow \Xi^-\overline{\Xi^0}), \\
A(\overline{B}^0 \rightarrow p\overline{p}) &= -A(\overline{B}_s^0 \rightarrow p\overline{\Sigma}^+), \\
A(B^- \rightarrow \Sigma^0\overline{\Sigma}^+) &= -\sqrt{2} A(\overline{B}^0 \rightarrow \Sigma^0\overline{\Sigma}^0), \\
A(B^- \rightarrow \Xi^-\overline{\Xi^0}) &= -A(\overline{B}^0 \rightarrow \Xi^-\overline{\Xi^-}), \quad (26)
\end{aligned}$$

for the $\Delta S = 0$ case, and

$$\begin{aligned}
\sqrt{3} A(B^- \rightarrow \Lambda\overline{p}) &= -\sqrt{2} A(B^- \rightarrow \Xi^0\overline{\Sigma}^+) \\
&+ A(B^- \rightarrow \Sigma^0\overline{p}), \\
A(B^- \rightarrow \Xi^-\overline{\Sigma^0}) &= \sqrt{3} A(B^- \rightarrow \Xi^-\overline{\Lambda}) \\
&+ \sqrt{2} A(B^- \rightarrow \Sigma^-\overline{n}), \\
A(\overline{B}^0 \rightarrow \Sigma^+\overline{p}) &= -A(\overline{B}_s^0 \rightarrow \Sigma^+\overline{\Sigma}^+), \quad (27)
\end{aligned}$$

TABLE V: Decomposition of $\overline{B} \rightarrow \mathcal{B}\overline{\mathcal{B}}$ amplitudes for $|\Delta S| = 1$ transitions in terms of tree and penguin amplitudes.

Mode	$T'_{1\mathcal{B}\overline{\mathcal{B}}}$	$T'_{2\mathcal{B}\overline{\mathcal{B}}}$	$T'_{3\mathcal{B}\overline{\mathcal{B}}}$	$T'_{4\mathcal{B}\overline{\mathcal{B}}}$	$P'_{1\mathcal{B}\overline{\mathcal{B}}}$	$P'_{2\mathcal{B}\overline{\mathcal{B}}}$
$B^- \rightarrow \Lambda\overline{p}$	$1/\sqrt{6}$	0	$1/\sqrt{6}$	0	$10/\sqrt{6}$	$-5/\sqrt{6}$
$\Xi^0\overline{\Sigma}^+$	-1	0	0	0	-5	0
$\Xi^-\overline{\Sigma}^0$	0	0	0	0	$-5/\sqrt{2}$	0
$\Xi^-\overline{\Lambda}$	0	0	0	0	$-5/\sqrt{6}$	$10/\sqrt{6}$
$\Sigma^-\overline{n}$	0	0	0	0	0	-5
$\Sigma^0\overline{p}$	$-1/\sqrt{2}$	0	$1/\sqrt{2}$	0	0	$-5/\sqrt{2}$
$B^0 \rightarrow \Lambda\overline{n}$	$1/\sqrt{6}$	$-1/\sqrt{6}$	$1/\sqrt{6}$	$-1/\sqrt{6}$	$10/\sqrt{6}$	$-5/\sqrt{6}$
$\Xi^-\overline{\Sigma}^-$	0	0	0	0	-5	0
$\Xi^0\overline{\Sigma}^0$	$1/\sqrt{2}$	0	0	0	$5/\sqrt{2}$	0
$\Xi^0\overline{\Lambda}$	$-1/\sqrt{6}$	$\sqrt{2}/3$	0	0	$-5/\sqrt{6}$	$10/\sqrt{6}$
$\Sigma^+\overline{p}$	0	-1	0	1	0	-5
$\Sigma^0\overline{n}$	$-1/\sqrt{2}$	$1/\sqrt{2}$	$1/\sqrt{2}$	$-1/\sqrt{2}$	0	$5/\sqrt{2}$
$B_s^0 \rightarrow \Lambda\overline{\Lambda}$	$-1/3$	$1/6$	$-1/3$	$1/6$	$-10/3$	$5/3$
$\Xi^0\overline{\Xi}^0$	-1	1	0	0	-5	5
$\Xi^-\overline{\Xi}^-$	0	0	0	0	-5	5
$\Sigma^+\overline{\Sigma}^+$	0	1	0	-1	0	5
$\Sigma^0\overline{\Sigma}^0$	0	$1/2$	0	$-1/2$	0	5
$\Sigma^-\overline{\Sigma}^-$	0	0	0	0	0	5
$\Lambda\overline{\Sigma}^0$	0	$-1/2\sqrt{3}$	0	$-1/2\sqrt{3}$	0	0
$\Sigma^0\overline{\Lambda}$	$1/\sqrt{3}$	$-1/2\sqrt{3}$	$-1/\sqrt{3}$	$1/2\sqrt{3}$	0	0

for the $|\Delta S| = 1$ case. More relations in the $|\Delta S| = 1$ case can be obtained by neglecting the sub-leading tree

contribution. We have

$$\begin{aligned}
A(B^- \rightarrow \Xi^-\overline{\Lambda}) &= A(\overline{B}^0 \rightarrow \Xi^0\overline{\Lambda}), \\
A(\overline{B}_s^0 \rightarrow \Xi^-\overline{\Xi}^-) &= A(\overline{B}_s^0 \rightarrow \Xi^0\overline{\Xi}^0), \\
\sqrt{2}A(B^- \rightarrow \Lambda\overline{p}) &= \sqrt{2}A(\overline{B}^0 \rightarrow \Lambda\overline{n}) = \sqrt{3}A(\overline{B}_s^0 \rightarrow \Lambda\overline{\Lambda}), \\
A(B^- \rightarrow \Xi^0\overline{\Sigma}^+) &= \sqrt{2}A(B^- \rightarrow \Xi^-\overline{\Sigma}^0) = A(\overline{B}^0 \rightarrow \Xi^-\overline{\Sigma}^-) = -\sqrt{2}A(\overline{B}^0 \rightarrow \Xi^0\overline{\Sigma}^0), \\
A(B^- \rightarrow \Sigma^-\overline{n}) &= \sqrt{2}A(B^- \rightarrow \Sigma^0\overline{p}) = A(\overline{B}^0 \rightarrow \Sigma^+\overline{p}) = -\sqrt{2}A(\overline{B}^0 \rightarrow \Sigma^0\overline{n}) \\
&= A(\overline{B}_s^0 \rightarrow \Sigma^+\overline{\Sigma}^+) = A(\overline{B}_s^0 \rightarrow \Sigma^0\overline{\Sigma}^0) = A(\overline{B}_s^0 \rightarrow \Sigma^-\overline{\Sigma}^-). \tag{28}
\end{aligned}$$

Rate relations implied by Eq. (28) are consistent with those obtained in Ref. [27]. In fact, Ref. [27] uses a generic SU(3) analysis and has three independent penguin amplitudes. One can reduce these amplitudes into two penguin amplitudes by imposing the OZI rule. As noted before the quark diagram approach is consistent with the OZI rule (see Eq. (25)). As a result, we have more relations.

To summarize, based solely on the flavor structure of H_W , we obtain one tree and one penguin amplitudes for the $\mathcal{D}\overline{\mathcal{D}}$ case; two tree and one penguin amplitudes for each of the $\mathcal{B}\overline{\mathcal{D}}$ and the $\mathcal{B}\overline{\mathcal{D}}$ case; four tree and two penguin amplitudes for the $\mathcal{B}\overline{\mathcal{B}}$ case. In principle, these amplitudes can be extracted from data. Various relations on decay rates as implied in Eqs. (12, 13, 18, 19, 21, 22, 26, 27, 28) are obtained and can be checked exper-

imentally. It should be pointed out that although we concentrate in tree and penguin amplitudes, the extension to include other contributions, such as W -exchange, electroweak penguin, weak annihilation and penguin annihilation amplitudes, is straightforward.

III. REDUCTION OF TOPOLOGICAL AMPLITUDES

Up to now we only make use of the flavor structure of the weak Hamiltonian. Amplitudes are decomposed topologically. In most cases, we need more than one tree and more than one penguin amplitudes. Although some relations are obtained, it is a long term experimental project to verify them. In fact, by taking into account

of the chirality structure of H_W , the number of independent amplitudes is reduced in the large m_B limit. It leads to more predictive results.

In general the charmless two-body decay amplitudes can be expressed as [12, 19]

$$\begin{aligned}\mathcal{A}(\overline{B} \rightarrow \mathcal{B}_1 \overline{\mathcal{B}}_2) &= \bar{u}_1(A_{\mathcal{B}\overline{\mathcal{B}}} + \gamma_5 B_{\mathcal{B}\overline{\mathcal{B}}})v_2, \\ \mathcal{A}(\overline{B} \rightarrow \mathcal{D}_1 \overline{\mathcal{B}}_2) &= i \frac{q^\mu}{m_B} \bar{u}_1^\mu(A_{\mathcal{D}\overline{\mathcal{B}}} + \gamma_5 B_{\mathcal{D}\overline{\mathcal{B}}})v_2, \\ \mathcal{A}(\overline{B} \rightarrow \mathcal{B}_1 \overline{\mathcal{D}}_2) &= i \frac{q^\mu}{m_B} \bar{u}_1(A_{\mathcal{B}\overline{\mathcal{D}}} + \gamma_5 B_{\mathcal{B}\overline{\mathcal{D}}})v_2^\mu, \\ \mathcal{A}(\overline{B} \rightarrow \mathcal{D}_1 \overline{\mathcal{D}}_2) &= \bar{u}_1^\mu(A_{\mathcal{D}\overline{\mathcal{D}}} + \gamma_5 B_{\mathcal{D}\overline{\mathcal{D}}})v_{2\mu} \\ &\quad + \frac{q^\mu q^\nu}{m_B^2} \bar{u}_1^\mu(C_{\mathcal{D}\overline{\mathcal{D}}} + \gamma_5 D_{\mathcal{D}\overline{\mathcal{D}}})v_{2\nu},\end{aligned}\quad (29)$$

where $q = p_1 - p_2$ and u^μ, v^μ are the Rarita-Schwinger vector spinors for a spin- $\frac{3}{2}$ particle. The vector spinors in various helicity states can be expressed as [40] $u_\mu(\pm\frac{3}{2}) = \epsilon_\mu(\pm 1)u(\pm\frac{1}{2})$, $u_\mu(\pm\frac{1}{2}) = (\epsilon_\mu(\pm 1)u(\mp\frac{1}{2}) + \sqrt{2}\epsilon_\mu(0)u(\pm\frac{1}{2}))/\sqrt{3}$, where $\epsilon_\mu(\lambda)$ and $u(s)$ are the usual polarization vector and spinor, respectively. By using $q \cdot \epsilon(\lambda)_{1,2} = \mp \delta_{\lambda,0} m_B p_c/m_{1,2}$, where p_c is the baryon momentum in the B rest frame, and the fact that $\epsilon_1^*(0) \cdot \epsilon_2(0) = (m_B^2 - m_1^2 - m_2^2)/2m_1m_2$ is the dominant term among $\epsilon_1^*(\lambda_1) \cdot \epsilon_2(\lambda_2)$, we have

$$\begin{aligned}\mathcal{A}(\overline{B} \rightarrow \mathcal{D}_1 \overline{\mathcal{B}}_2) &= -i\sqrt{\frac{2}{3}} \frac{p_c}{m_1} \bar{u}_1(A_{\mathcal{D}\overline{\mathcal{B}}} + \gamma_5 B_{\mathcal{D}\overline{\mathcal{B}}})v_2, \\ \mathcal{A}(\overline{B} \rightarrow \mathcal{B}_1 \overline{\mathcal{D}}_2) &= i\sqrt{\frac{2}{3}} \frac{p_c}{m_2} \bar{u}_1(A_{\mathcal{B}\overline{\mathcal{D}}} + \gamma_5 B_{\mathcal{B}\overline{\mathcal{D}}})v_2, \\ \mathcal{A}(\overline{B} \rightarrow \mathcal{D}_1 \overline{\mathcal{D}}_2) &\simeq \frac{m_B^2}{3m_1m_2} \bar{u}_1(A'_{\mathcal{D}\overline{\mathcal{D}}} + \gamma_5 B'_{\mathcal{D}\overline{\mathcal{D}}})v_2,\end{aligned}\quad (30)$$

where $A'_{\mathcal{D}\overline{\mathcal{D}}} = A_{\mathcal{D}\overline{\mathcal{D}}} - 2(p_c/m_B)^2 C_{\mathcal{D}\overline{\mathcal{D}}}$, $B'_{\mathcal{D}\overline{\mathcal{D}}} = B_{\mathcal{D}\overline{\mathcal{D}}} - 2(p_c/m_B)^2 D_{\mathcal{D}\overline{\mathcal{D}}}$ and decuplets are in $h = \pm\frac{1}{2}$ helicity states. Note that the first two equations are exact while the last one holds in the $m_B^2 \gg m_{1,2}^2, m_1m_2$ limit. For these amplitudes to have the same $m_B^2 = (p_1 + p_2)^2$ behavior in the large m_B^2 limit, the extra factor of p_c and m_B in Eq. (30) should be suitably compensated by the $1/m_B^2$ power of the corresponding A and B terms. For all four $\overline{B} \rightarrow \mathbf{B}_1 \overline{\mathbf{B}}_2$ ($\mathbf{B}\overline{\mathbf{B}} = \mathcal{B}\overline{\mathcal{B}}, \mathcal{D}\overline{\mathcal{B}}, \mathcal{B}\overline{\mathcal{D}}, \mathcal{D}\overline{\mathcal{D}}$) decays, we can effectively use

$$\mathcal{A}(\overline{B} \rightarrow \mathbf{B}_1 \overline{\mathbf{B}}_2) = \bar{u}_1(A + \gamma_5 B)v_2, \quad (31)$$

as the decay amplitudes.

The chiral structure of weak interaction provide further information on A and B . For example, in the $\Delta S = 0$ processes, we have $b \rightarrow u_L \bar{u}_R d_L$ and $b \rightarrow d_L q_L(R) \bar{q}_R(L)$ decays. The produced d_L quark is left-handed in both tree and penguin decays. Furthermore, as strong interaction is chirality conserving, the pop up quark pair $q' \bar{q}'$ should be $q'_L \bar{q}'_R$ or $q'_R \bar{q}'_L$. From the conservation of helicity, the produced baryon and anti-baryon must be in left-helicity states. To be more specify, we take the $\overline{B}_s^0 \rightarrow \mathbf{B}\overline{\mathbf{B}}$

decay as an example. According to the above argument, the final state (anti-)baryons should have $u_L d_L q'_R$ ($\bar{q}'_L \bar{u}_R \bar{s}_L$) configuration from the tree $b \rightarrow u_L \bar{u}_R d_L$ decay and $d_L q_L(R) q'_R(L)$ ($\bar{q}'_L(R) \bar{q}_R(L) \bar{s}_L$) configuration from the penguin $b \rightarrow d_L q_L(R) \bar{q}_R(L)$ decay. In the large m_B limit, as the spinor helicity identify to chirality, we should have $B \rightarrow -A$ in the above equation.

The number of independent topological amplitudes is reduced in the large m_B limit. The corresponding asymptotic relations are derived in the appendix. Some of the reduction can be understood by using the chirality structure of weak interaction, the helicity argument and the anti-symmetry property of the Λ wave function.

The $b \rightarrow u_L \bar{u}_R d_L$ process have final state u and d quarks both with left-handed chirality or helicity (as light quark masses are neglected). It is well known that in the Λ wave function the u and d quarks have opposite helicity (as shown in Eq. (A2)). Therefore, the tree amplitudes in the $\Delta S = 0$, $\overline{B} \rightarrow \Lambda \overline{\mathcal{D}}, \Lambda \overline{\mathcal{B}}$ decays should be vanishing. As shown in Table II and Table IV these amplitudes are proportional to $2T_{1\mathcal{B}\overline{\mathcal{D}}} - T_{2\mathcal{B}\overline{\mathcal{D}}}$ and $2T_{1\mathcal{B}\overline{\mathcal{B}}} - T_{3\mathcal{B}\overline{\mathcal{B}}}, 2T_{2\mathcal{B}\overline{\mathcal{B}}} - T_{4\mathcal{B}\overline{\mathcal{B}}}$, respectively. We should have

$$T_{1\mathcal{B}\overline{\mathcal{D}}}^{(\prime)} = \frac{1}{2} T_{2\mathcal{B}\overline{\mathcal{D}}}^{(\prime)}, \quad (32)$$

and

$$T_{1\mathcal{B}\overline{\mathcal{B}}}^{(\prime)} = \frac{1}{2} T_{3\mathcal{B}\overline{\mathcal{B}}}^{(\prime)}, \quad T_{2\mathcal{B}\overline{\mathcal{B}}}^{(\prime)} = \frac{1}{2} T_{4\mathcal{B}\overline{\mathcal{B}}}^{(\prime)}. \quad (33)$$

Although above relations are obtained in the $\Delta S = 0$ case, as shown in the appendix, they also hold in the $|\Delta S| = 1$ case.

Furthermore, we note that there should be no penguin contribution to the $\overline{B}^0 \rightarrow \Lambda \overline{\Lambda}$ decay amplitude. In the penguin type $b \rightarrow d_L$ decay, the quark content of the produced Λ should be $d_L u_R s_L$, since the u d pair of the Λ wave function is in a spin zero configuration. From the helicity (or chirality) conservation, the correlated anti-baryon is in a left-handed helicity state with quark content $\bar{d}_L \bar{u}_L \bar{s}_R$, which cannot match to the wave function of $\overline{\Lambda}$ and resulting a vanishing penguin contribution on the $\overline{B}^0 \rightarrow \Lambda \overline{\Lambda}$ mode. As shown in Table IV, its penguin amplitude is proportional to $P_{1\mathcal{B}\overline{\mathcal{B}}} - 5P_{2\mathcal{B}\overline{\mathcal{B}}}$ and we should have

$$P_{1\mathcal{B}\overline{\mathcal{B}}}^{(\prime)} = 5P_{2\mathcal{B}\overline{\mathcal{B}}}^{(\prime)}. \quad (34)$$

According to the decomposition shown in Eq. (25), this relation can be expressed by $(P_D/P_F) \rightarrow (3/2)$, which is consistent with the asymptotic relation on the baryon scalar and pseudoscalar form factors obtained in Ref. [15].

There is no constraint from processes involving $\overline{\Lambda}$ final states in the $\overline{B} \rightarrow \mathcal{D}\overline{\mathcal{B}}$ decays and we still have two independent tree amplitudes in $\overline{B} \rightarrow \mathcal{B}\overline{\mathcal{B}}$ decays. Asymptotic relations lead to further reduction,

$$T_{1\mathcal{D}\overline{\mathcal{B}}}^{(\prime)} = -T_{2\mathcal{D}\overline{\mathcal{B}}}^{(\prime)}. \quad (35)$$

and

$$T_{1B\bar{B}}^{(\prime)} = -T_{2B\bar{B}}^{(\prime)}, \quad (36)$$

in the large m_B limit.

It is interesting to note that in Ref. [36] the octet-octet and octet-decuplet systems are related asymptotically. Similarly, we have

$$\begin{aligned} T^{(\prime)} &= T_{D\bar{D}}^{(\prime)} = T_{1B\bar{D}}^{(\prime)} = T_{1D\bar{B}}^{(\prime)} = T_{1B\bar{B}}^{(\prime)}, \\ P^{(\prime)} &= P_{D\bar{D}}^{(\prime)} = P_{B\bar{D}}^{(\prime)} = P_{D\bar{B}}^{(\prime)} = P_{1B\bar{B}}^{(\prime)}, \end{aligned} \quad (37)$$

in the large m_B limit. In that limit, we need only one tree and one penguin amplitudes under the quark diagram approach for all four classes of charmless two-body baryonic modes. In the next section, we will use the above equation as an approximation to study the decay rates. It should be verified by data that whether this is a good approximation or not.

IV. PHENOMENOLOGICAL DISCUSSION

In this section, we discuss the phenomenology of charmless two-body baryonic modes by using the formalism developed in previous sections. Since none of the charmless two-body baryonic decay is observed so far, we suggest some prominent modes for experimental searches. This section is divided into two parts, discussing tree-dominated and penguin-dominated modes, respectively. We summarize our results at the end of this section.

A. Tree-dominated modes

For $\Delta S = 0$ modes, we expect tree amplitudes to dominate. We can estimate their relative rates by neglecting penguin contribution. Rates are normalized to the $\bar{B}^0 \rightarrow p\bar{p}$ rate. As noted before, a simple scaling of $|V_{ub}/V_{cb}|^2$ on the $\bar{B}^0 \rightarrow \Lambda_c^+ \bar{p}$ decay rate hints at a $\sim 10^{-7}$ rate for the charmless case [6]. A pole model calculation also gives $\mathcal{B}(\bar{B}^0 \rightarrow p\bar{p}) = 1.1 \times 10^{-7}$ [12]. For illustration, we take $\mathcal{B}(\bar{B}^0 \rightarrow p\bar{p}) = 1 \times 10^{-7}$ as the reference rate for these tree-dominated decay rates.

As noted in the end of the previous section, we use the asymptotic relations stated in Eqs. (32–37) for tree and penguin amplitudes shown in Tables I–IV. Hadron masses and $B^{-,0}$, B_s lifetimes taken from Ref. [8] are used to indicate some SU(3) breaking effects. Results obtained are given in Table VI. For comparison, we quote results of pole model [12], diquark mode [23] and sum rule [21] calculations in the subsiding order in parentheses. We normalize the tree contributed $\mathcal{B}_T(\bar{B}^0 \rightarrow p\bar{p})$ of Ref. [12] and Ref. [21] to 1×10^{-7} . Note that the $\bar{B}^0 \rightarrow p\bar{p}$ rate only decreased by 16% by including penguin contributions in Ref. [23]. The tree-penguin interference effect is not prominent. We will wait for data before carry out a detail study of the tree-penguin interference effect.

Rate relations shown in Table VI are consistent with Eqs. (12, 18, 21, 22, 26). We find that the tree-dominated $\bar{B} \rightarrow N\bar{\Delta}$ modes have the structure

$$\begin{aligned} \mathcal{B}(B^- \rightarrow p\bar{\Delta}^{++}) &\simeq 3\mathcal{B}(\bar{B}^0 \rightarrow p\bar{\Delta}^+) \\ &\simeq 3\mathcal{B}(B^- \rightarrow n\bar{\Delta}^+) \simeq 3\mathcal{B}(\bar{B}^0 \rightarrow n\bar{\Delta}^0), \end{aligned} \quad (38)$$

which is consistent with Refs. [12, 19], while the $\mathcal{B}(\bar{B} \rightarrow N\bar{\Delta})/\mathcal{B}(\bar{B}^0 \rightarrow p\bar{p})$ ratios are smaller than those obtained in Ref. [12] by a factor of two. We have $\mathcal{B}(\bar{B}^0 \rightarrow p\bar{p}) \simeq \mathcal{B}(B^- \rightarrow p\bar{n})$, which is close to the sum-rule result [21]. On the other hand, our prediction on $\mathcal{B}(\bar{B}^0 \rightarrow n\bar{n}) : \mathcal{B}(\bar{B}^0 \rightarrow p\bar{p}) \simeq 4 : 1$ is different from all quoted earlier results. This different may be related to the following fact. It is easy to see from Table IV and Eqs. (33, 36) that by neglecting the sub-leading penguin contribution we have

$$A(B^- \rightarrow n\bar{p}) - A(\bar{B}^0 \rightarrow p\bar{p}) = A(\bar{B}^0 \rightarrow n\bar{n}). \quad (39)$$

The origin of the above equation is the corresponding e_T coefficients shown in Table IX. Note that the above equation is different from the $\Delta I = \frac{1}{2}$ rule relation [12, 19], which implies $|A(\bar{B}^0 \rightarrow p\bar{p}) - A(\bar{B}^0 \rightarrow n\bar{n})| = |A(B^- \rightarrow n\bar{p})|$. In fact, a highly suppressed $\mathcal{B}(B^- \rightarrow \pi^-\pi^0)/\mathcal{B}(\bar{B}^0 \rightarrow \pi^+\pi^-)$ ratio is followed from the $\Delta I = \frac{1}{2}$ rule in the charmless mesonic sector. Although the present data is still fluctuating, it suggests $\mathcal{B}(\pi^-\pi^0)/\mathcal{B}(\pi^+\pi^-) \sim 1$ [41]. We do not worry about the deviation of the $\Delta I = \frac{1}{2}$ rule in Eq. (39) at this stage. Note that we have $\mathcal{B}(\bar{B}^0 \rightarrow \Lambda\bar{\Lambda}) = 0$. As shown in the previous section, the vanishing of the $\bar{B}^0 \rightarrow \Lambda\bar{\Lambda}$ rate is due to the anti-symmetric property of the Λ wave function and the chirality argument in the large m_B limit. This mode provides a useful check of the approximation made.

Upper limits on $\bar{B}^0 \rightarrow p\bar{p}$, $\Lambda\bar{\Lambda}$ and $B^- \rightarrow \Lambda\bar{p}$ are obtained [7] (see, Eq. (2)). Some observed three-body modes [3–5] also provide constraints. To discuss the feasibility of experimental observation, it is useful to recall that $\mathcal{B}(\Sigma^0 \rightarrow \Lambda\gamma) \simeq 1$, $\mathcal{B}(\Xi \rightarrow \Lambda\pi) \sim 1$, $\mathcal{B}(\Delta^+ \rightarrow p\pi^0) \simeq \frac{2}{3}$, $\mathcal{B}(\Delta^0 \rightarrow p\pi^-) \simeq \frac{1}{3}$ and $\mathcal{B}(\Sigma^* \rightarrow \Lambda\pi) = 88\%$ [8].

As shown in the first column of Table VI, there are ten \bar{B}^0 decay modes having rates larger than the reference $\bar{B}^0 \rightarrow p\bar{p}$ rate. We can search for the $\Sigma^0\bar{\Lambda}$ mode, which has a rate about three times of the $p\bar{p}$ rate and clear signature for reconstruction. Up to now, most experimental searches in baryonic modes do not involve π^0 in reconstruction. With one π^0 in the final states, we can search for $p\bar{\Delta}^+$, $\Delta^+\bar{p}$, $\Sigma^0\bar{\Sigma}^0$ and $\Sigma^*\bar{\Lambda}$ modes, which have rates about twice of the $\bar{B}^0 \rightarrow p\bar{p}$ rate. Note that $\bar{B}^0 \rightarrow n\bar{n}$, $\Delta^0\bar{n}$ decays have rates larger than the $p\bar{p}$ rate by factors of four and eight, respectively, but require \bar{n} or even n in detection.

We now turn to B^- decay modes as shown in the second column of Table VI. One should search for the $\Delta^+\bar{\Delta}^{++}$ mode, which have the largest rate, $\mathcal{B}(B^- \rightarrow$

TABLE VI: Decay rates for $\Delta S = 0$ tree-dominated modes. We consider only tree amplitude contribution. Rates are normalized to $\mathcal{B}(\bar{B}^0 \rightarrow p\bar{p})$. For comparison, we show results of pole model [12], diquark mode [23] and sum rule [21] calculations in the subsidting order in parentheses.

Mode	$\mathcal{B}(10^{-7})$	Mode	$\mathcal{B}(10^{-7})$	Mode	$\mathcal{B}(10^{-7})$
$B^0 \rightarrow p\bar{p}$	1 ^a	$(1.1, 0.84, 1)$	$B^- \rightarrow n\bar{p}$	1.09	$(5.0, 0, 0.6)$
$n\bar{n}$	4.00	$(1.2, 0.84, 0.3)$	$\Sigma^0\bar{\Sigma}^+$	1.99	
$\Lambda\bar{\Lambda}$	0	$(0, 0.38, \text{---})$	$p\bar{\Delta}^{++}$	6.19	$(14, 0.63, 0.25)$
$\Sigma^0\bar{\Lambda}$	2.79		$n\bar{\Delta}^+$	2.06	$(4.6, 0.70, \text{---})$
$\Sigma^0\bar{\Sigma}^0$	0.91		$\Sigma^0\bar{\Sigma}^{*+}$	3.81	
$p\bar{\Delta}^+$	1.90	$(4.3, 0.28, 0.1)$	$\Delta^0\bar{p}$	2.06	
$n\bar{\Delta}^0$	1.90	$(4.3, 0.28, \text{---})$	$\Sigma^{*0}\bar{\Sigma}^+$	0.95	
$\Sigma^0\bar{\Sigma}^{*0}$	1.75		$\Delta^+\bar{\Delta}^{++}$	11.72	
$\Delta^+\bar{p}$	1.90		$\Delta^0\bar{\Delta}^+$	3.91	
$\Delta^0\bar{n}$	7.60		$\Sigma^{*0}\bar{\Sigma}^{*+}$	1.82	
$\Sigma^{*0}\bar{\Lambda}$	1.34				
$\Sigma^{*0}\bar{\Sigma}^0$	0.44				
$\Delta^+\bar{\Delta}^+$	3.60				
$\Delta^0\bar{\Delta}^0$	3.60				
$\Sigma^{*0}\bar{\Sigma}^{*0}$	0.84				

^aWe take $\mathcal{B}(\bar{B}^0 \rightarrow p\bar{p}) = 1 \times 10^{-7}$ as a reference rate.

$\Delta^+\bar{\Delta}^{++}) = 11.7 \mathcal{B}(\bar{B}^0 \rightarrow p\bar{p})$, and only reduces $\sim 30\%$ in producing $p\pi^0\bar{p}\pi^-$ final state. Two modes, $p\bar{\Delta}^{++}$ and $\Delta^0\bar{p}$, can decay to the all charged $p\bar{p}\pi^-$ final state. They have rates six and two times of $\mathcal{B}(\bar{B}^0 \rightarrow p\bar{p})$ and are searchable. Their rates are within the tree-body (total) rate constraint, $\mathcal{B}(p\bar{p}\pi^-) = (3.06^{+0.73}_{-0.62} \pm 0.40) \times 10^{-6}$ [4], and should be accessible.

For the B_s case, one needs all charge track for detection. As shown in the third column of Table VI the $p\bar{\Sigma}^{*+}$ and $\Delta^0\bar{\Lambda}$ modes have rates of one to three times of $\mathcal{B}(p\bar{p})$ and should be searchable.

There are some pure-tree modes in $|\Delta S| = 1$ processes. We use $T' = TV_{us}^*/V_{ud}^*$ to estimate their rates and obtain $\mathcal{B}(B^- \rightarrow \Lambda\bar{\Delta}^+) = 0.15 \times 10^{-7}$ and $\mathcal{B}(\bar{B}_s^0 \rightarrow \Lambda\bar{\Sigma}^{*0}, \Sigma^{*0}\bar{\Lambda}) = 0.07 \times 10^{-7}$, which are quite small as expected. There are some pure-penguin modes in the $\Delta S = 0$ process as shown in Tables I–IV. Their rates are suppressed and will be briefly discussed in the next sub-section.

B. Penguin-dominated modes

The relative rates for penguin-dominated modes can be obtained similarly as in the previous subsection, but instead of neglecting penguin amplitudes we neglect tree amplitudes. We use $B^- \rightarrow \Lambda\bar{p}$ as a reference mode. The present experimental limit is $\mathcal{B}(B^- \rightarrow \Lambda\bar{p}) < 2.2 \times 10^{-6}$ [7]. On the theoretical side, a recent pole model calculation gives $\mathcal{B}(B^- \rightarrow \Lambda\bar{p}) = 2\mathcal{B}(\bar{B}^0 \rightarrow p\bar{p}) = 2.2 \times 10^{-7}$ [12], while a diquark model calculation gives $\mathcal{B}(B^- \rightarrow \Lambda\bar{p}) = 0.18\mathcal{B}(\bar{B}^0 \rightarrow p\bar{p})$ [23]. Due to the controversial situation of these predictions, we use $\mathcal{B}(B^- \rightarrow \Lambda\bar{p}) = 1 \times 10^{-7}$ as a convenient reference rate

for illustration. In Table VII we show rates for penguin-dominated modes, while rates for pure-penguin modes are given in Table VIII. Rate ratios are consistent with Eqs. (13, 19, 22, 27, 28). For comparison, we show results of pole model [12], diquark mode [23] and sum rule [21] calculations, in the subsidting order in parentheses. The diquark and sum rule results are normalized as before.

The $\mathcal{B}(\bar{B}^0 \rightarrow \Lambda\bar{n})/\mathcal{B}(B^- \rightarrow \Lambda\bar{p})$ ratio is similar to those obtained in pole model and diquark model calculations [12, 23], while the $\mathcal{B}(\bar{B}^0 \rightarrow \Sigma^+\bar{p})/\mathcal{B}(B^- \rightarrow \Lambda\bar{p})$ ratio is consistent with the pole model result [12]. For other cases, we have quite different predictions.

As shown in Table VII, the $B^- \rightarrow \Lambda\bar{p}$ decay is still the best mode to search for. Other modes may have much smaller rates or much lower detection efficiencies. For example, although the $B^- \rightarrow \Sigma^0\bar{p}$ decay signature is easy to identify, its rate is too small to search for. This smallness as compared to the $\Lambda\bar{p}$ rate can be traced to the e_P ratio $(-1/3\sqrt{2} : \sqrt{3/2})$ as shown in Table IX. Note that the same ratio is obtained in the $\Lambda\bar{p}$ vs. $\Sigma^0\bar{p}$ (pseudo)scalar form factors in the asymptotic limit [15]. The resulting prediction, $\mathcal{B}(\Lambda\bar{p}\pi^-) > \mathcal{B}(\Sigma^0\bar{p}\pi^-)$, is supported by data [5]. The $B^- \rightarrow \Xi^0\bar{\Sigma}^+$ rate is about twice the $\Lambda\bar{p}$ rate, but we need two π^0 in reconstruction. Note that an all charged final state can be found in the $B^- \rightarrow \Sigma^{*+}\bar{\Delta}^{++} \rightarrow \Lambda\pi^+\bar{p}\pi^-$ decay with only 10% reduction in rate.

The penguin-dominated \bar{B}^0 decay rates are shown in the second column of Table VII. In general their rate are within $\mathcal{B}(B^- \rightarrow \Lambda\bar{p})$. We note that the $\Sigma^0\bar{\Delta}^0$ final state has one third of chance to decay to $\Sigma^0\bar{p}\pi^-$ and the rate is within the three-body total rate constraint ($\mathcal{B}(\Sigma^0\bar{p}\pi^-) < 3.8 \times 10^{-6}$ at 90% confidence level [5]). For the B_s case, the $\Lambda\bar{\Lambda}$ mode is the most searchable one.

TABLE VII: Decay rates for $|\Delta S| = 1$ penguin-dominated modes. We consider only penguin amplitude contribution. Rates are normalize to $\mathcal{B}(B^- \rightarrow \Lambda\bar{p})$. For comparison, we show results of pole model [12], diquark mode [23] and sum rule [21] calculations in the subsiding order in parentheses.

Mode	$\mathcal{B}(10^{-7})$	Mode	$\mathcal{B}(10^{-7})$	Mode	$\mathcal{B}(10^{-7})$
$B^- \rightarrow \Lambda\bar{p}$	1 ^b	$(2.2, 0.18, < 3.8)$	$\bar{B}^0 \rightarrow \Sigma^+\bar{p}$	0.07	$(0.2, 0.88, 7.5)$
$\Sigma^0\bar{p}$	0.04	$(0.6, 0.18, 3.8)$	$\Lambda\bar{n}$	0.92 ^c	$(2.1, 0.21, —)$
$\Xi^0\bar{\Sigma}^+$	1.70		$\Sigma^0\bar{n}$	0.03 ^c	$(—, 0.21, —)$
$\Sigma^0\bar{\Delta}^+$	0.28	$(—, 0.08, —)$	$\Xi^0\bar{\Sigma}^0$	0.78	
$\Xi^0\bar{\Sigma}^{*+}$	0.13		$\Sigma^0\bar{\Delta}^0$	0.26	$(—, 0.17, —)$
$\Sigma^+\bar{\Delta}^{++}$	0.42	$(2.0, 1.10, 7.5)$	$\Xi^0\bar{\Sigma}^{*0}$	0.06	
$\Sigma^{*0}\bar{p}$	0.07		$\Sigma^+\bar{\Delta}^+$	0.13	$(0.6, 0.57, 7.5)$
$\Xi^{*0}\bar{\Sigma}^+$	0.13		$\Sigma^{*0}\bar{n}$	0.06	
$\Sigma^{*0}\bar{\Delta}^+$	0.53		$\Sigma^{*+}\bar{p}$	0.13	
$\Sigma^{*+}\bar{\Delta}^{++}$	0.80		$\Xi^{*0}\bar{\Lambda}$	0.20	
$\Xi^{*0}\bar{\Sigma}^{*+}$	0.98		$\Xi^{*0}\bar{\Sigma}^0$	0.06	
			$\Sigma^{*0}\bar{\Delta}^0$	0.49	
			$\Sigma^{*+}\bar{\Delta}^+$	0.24	
			$\Xi^{*0}\bar{\Sigma}^{*0}$	0.45	

^bWe take $\mathcal{B}(B^- \rightarrow \Lambda\bar{p}) = 1 \times 10^{-7}$ as our reference rate.

^cThese modes may have large tree contributions. See text for detail discussion.

TABLE VIII: Rates (normalized to $\mathcal{B}(B^- \rightarrow \Lambda\bar{p}) = 1 \times 10^{-7}$) for pure penguin modes in the $|\Delta S| = 1$ process. For comparison we show results of Ref. [12] in the parenthesis.

Mode	$\mathcal{B}(10^{-7})$	Mode	$\mathcal{B}(10^{-7})$	Mode	$\mathcal{B}(10^{-7})$
$B^- \rightarrow \Xi^-\bar{\Sigma}^0$	0.85	$\bar{B}^0 \rightarrow \Xi^-\bar{\Sigma}^-$	1.56	$\bar{B}_s^0 \rightarrow \Xi^-\bar{\Xi}^-$	0.98
$\Xi^-\bar{\Lambda}$	0.10	$\Xi^0\bar{\Lambda}$	0.10	$\Sigma^-\bar{\Sigma}^-$	0.06
$\Sigma^-\bar{n}$	0.07	$\Xi^-\bar{\Sigma}^{*-}$	0.12	$\Sigma^-\bar{\Sigma}^{*-}$	0.12
$\Xi^-\bar{\Sigma}^{*0}$	0.06	$\Sigma^-\bar{\Delta}^-$	0.38	$\Xi^-\bar{\Xi}^{*-}$	0.12
$\Sigma^-\bar{\Delta}^0$	0.14 (0.7)	$\Xi^{*-}\bar{\Sigma}^-$	0.12	$\Sigma^{*-}\bar{\Sigma}^-$	0.12
$\Sigma^*\bar{n}$	0.14	$\Omega^-\bar{\Xi}^-$	0.33	$\Xi^{*-}\bar{\Xi}^-$	0.12
$\Xi^{*-}\bar{\Lambda}$	0.20	$\Sigma^{*-}\bar{\Delta}^-$	0.73	$\Sigma^{*-}\bar{\Sigma}^{*-}$	0.24
$\Xi^{*-}\bar{\Sigma}^0$	0.06	$\Xi^{*-}\bar{\Sigma}^{*-}$	0.90	$\Xi^{*-}\bar{\Xi}^{*-}$	0.88
$\Omega^-\bar{\Xi}^0$	0.36	$\Omega^-\bar{\Xi}^*$	0.62	$\Omega^-\bar{\Omega}^-$	1.82
$\Sigma^{*-}\bar{\Delta}^0$	0.27				
$\Xi^{*-}\bar{\Sigma}^{*0}$	0.49				
$\Omega^-\bar{\Xi}^{*0}$	0.68				

We note that some modes may have large tree contributions. For example, as one can see from Table V and Eqs. (33, 36) that $\bar{B}^0 \rightarrow \Lambda\bar{n}$, $\Sigma^0\bar{n}$ amplitudes have relatively large T' coefficients. By using $T' = TV_{us}^*/V_{ud}^*$, we have $\mathcal{B}_T(\bar{B}^0 \rightarrow \Lambda\bar{n}, \Sigma^0\bar{n}) = (0.12, 0.07) \mathcal{B}(\bar{B}^0 \rightarrow p\bar{p})$ from tree contributions. For these modes, tree-penguin interference may affects their rates dramatically. For example, by including tree contribution in $\bar{B}^0 \rightarrow \Sigma^0\bar{n}$ decay, Ref. [23] obtains a factor of five enhancement of an earlier calculation [22]. As one can see from Tables I–V and asymptotic relations that other $|\Delta S| = 1$ modes do not have such a large relative tree contribution. The tree-penguin interference for them are expected to be much milder.

Rates for pure-penguin modes are shown in Table VIII. They are in general not favorable than the $B^- \rightarrow \Lambda\bar{p}$

mode. The largest mode of pure-penguin B^- decays is $\Xi^-\bar{\Sigma}^0$ and one may search for it after the observation of the $\Lambda\bar{p}$ mode. Although the $\bar{B}^0 \rightarrow \Xi^-\bar{\Sigma}^-$ rate is 1.6 times of $\Lambda\bar{p}$ rate, we need $\Lambda\pi^-\bar{n}\pi^+$ for detection. One may have chance to search for $\bar{B}_s^0 \rightarrow \Xi^-\bar{\Xi}^-$, $\Omega^-\bar{\Omega}^-$ decays through $\Lambda\pi^-\bar{\Lambda}\pi^+$, $\Lambda K^-\bar{\Lambda}K^+$ final states, respectively.

As noted in the end of the previous subsection, there are some pure penguin decays in $\Delta S = 0$ processes. We can estimate their rate by using $P = P'V_{td}^*/V_{ts}^*$. Their rates are typically of 10^{-9} and even the largest rate, $\mathcal{B}(\bar{B}^0 \rightarrow \Delta^-\bar{\Delta}^-) \simeq 9 \times 10^{-9}$, is still undetectable.

We give a summary of our suggestions before ending this section. We find that in $\Delta S = 0$ processes, in addition of the $\bar{B}^0 \rightarrow p\bar{p}$ search, it is useful to search for the $\bar{B}^0 \rightarrow \Sigma^0\bar{\Lambda}$ decay and $B^- \rightarrow \Delta^+\bar{\Delta}^{++}$, $p\bar{\Delta}^{++}$, $\Delta^0\bar{p}$ decays. In particular, the $\Delta^+\bar{\Delta}^{++}$ rate is larger than

the $p\bar{p}$ rate by one order of magnitude. It could be the first charmless two-body baryonic mode to appear. For $|\Delta S| = 1$ processes, the $B^- \rightarrow \Lambda\bar{p}$ decay is still the best mode to search for. After the observation of any of the above mention modes, one should also search for other sub-dominated modes, such as $\bar{B}^0 \rightarrow p\Delta^+$, $\Delta^+\bar{p}$, $\Sigma^0\bar{\Sigma}^0$, $\Sigma^{*0}\bar{\Lambda}$, $\Xi^-\bar{\Sigma}^-$ and $B^- \rightarrow \Xi^-\bar{\Sigma}^0$, $\Sigma^{*+}\bar{\Delta}^{++}$ decays. For the B_s case, as all charged tracks final states are required for detection, one can search for the $p\bar{\Sigma}^{(*)+}$, $\Delta^0\bar{\Lambda}$, $\Xi^-\bar{\Xi}^-$ and $\Omega^-\bar{\Omega}^-$ modes, which have rates compatible to $\bar{B}^0 \rightarrow p\bar{p}$ or $B^- \rightarrow \Lambda\bar{p}$ decay rates. We note that although rates shown in Table VI seems more promising than those shown Table VII and Table VIII, the reference $B^- \rightarrow \Lambda\bar{p}$ rate may be greater than the reference $\bar{B}^0 \rightarrow p\bar{p}$ rate and resulting a different prospect. Nevertheless, there are many promising modes, as good as the $p\bar{p}$ mode, in $\Delta S = 0$ processes, while the Λp mode is still be best candidate in $|\Delta S| = 1$ processes.

V. DISCUSSION AND CONCLUSION

In this work, we use a quark diagram approach to classify various contributions on charmless two-body baryonic B decays. This approach is closely related to flavor symmetry, since a quark diagram is a representation of it. Relations on decay amplitudes are obtained. As noted in Sec. II, our results are consistent with some generic SU(3) results with the OZI rule imposed. Since we match baryon and qqq flavors in the beginning, the OZI rule should be satisfied. In this sense, we may view the diagrammatic approach as an flavor symmetry approach with the OZI-rule constraint.

We concentrated on tree and strong penguin contributions in decay rates. Other contributions are sub-leading and can be included later. For example, the electroweak penguin contribution can be included by a simple redefinition of tree and strong penguin amplitudes as in the mesonic case [34]. Some contributions, such as weak exchange and annihilation topologies, can be included by extending Eq. (11) to other cases, but they are expected to be $1/m_B^2$ suppressed. Amplitude relations are obtained by considering tree and penguin contributions.

There are in general more than one tree and more than one penguin amplitudes to describe charmless two-body baryonic decays. Reduction in the number of independent amplitudes can be achieved by considering the chirality nature of weak interaction and the large m_B limit. Some relations can be understood by using the anti-symmetry behavior of the Λ wave function. An interesting check is the experimental verification of the vanishing or highly suppressed $\bar{B}^0 \rightarrow \Lambda\bar{\Lambda}$ rate. As in Ref. [36], the octet-octet and octet-decuplet systems are related asymptotically, we need only one tree and one penguin amplitudes to describe charmless two-body baryonic decays. The followed results are very predictive and can be checked by experiments.

We suggest some prominent modes to search for. In

$\Delta S = 0$ processes, there are many promising modes. In addition of the $\bar{B}^0 \rightarrow p\bar{p}$ search, it is useful to search for $\bar{B}^0 \rightarrow \Sigma^0\bar{\Lambda}$ decay and $B^- \rightarrow \Delta^+\bar{\Delta}^{++}$, $p\bar{\Delta}^{++}$, $\Delta^0\bar{p}$ decays. For $|\Delta S| = 1$ processes, the $B^- \rightarrow \Lambda\bar{p}$ decay is still the best mode to search for. After the observation of any of the above mention modes, one should also search for other sub-dominated modes. For the B_s case, one can search for the $p\bar{\Sigma}^{(*)+}$, $\Delta^0\bar{\Lambda}$, $\Xi^-\bar{\Xi}^-$ and $\Omega^-\bar{\Omega}^-$ decay modes. Although the above suggestions are obtained by considering the dominant contributions, we do not expect large modification of relative rate ratio in most cases. The tree-penguin interference effects can be included later after the appearance of data.

To conclude, we use a quark diagram approach to study charmless two-body baryonic decays. The topological amplitudes can be extracted from data. We further apply asymptotic relations to reduce the number of independent topological amplitudes and obtained predictive results. We have pointed out several promising modes to be added to the present experimental searching list. The discovery of any one of them should be followed by a bunch of other modes.

Acknowledgments

The author thanks H.-Y. Cheng, H.-C. Huang and H.-n. Li for discussions. This work is supported by the National Science Council of R.O.C. under Grant NSC-91-2811-M-002-043, the MOE CosPA Project, and the BCP Topical Program of NCTS.

APPENDIX A: ASYMPTOTIC RELATIONS IN THE LARGE m_B LIMIT

We follow Ref. [15, 36] to obtain the asymptotic relations stated in Sec. III. As noted we only need to consider helicity $\pm\frac{1}{2}$ states. The wave function of a right-handed (helicity = $\frac{1}{2}$) baryon can be expressed as

$$|\mathbf{B}; \uparrow\rangle \sim \frac{1}{\sqrt{3}}(|\mathbf{B}; \uparrow\downarrow\uparrow\rangle + |\mathbf{B}; \uparrow\uparrow\downarrow\rangle + |\mathbf{B}; \downarrow\uparrow\uparrow\rangle), \quad (A1)$$

i.e. composed of 13-, 12- and 23-symmetric terms, respectively. For $\mathbf{B} = \Delta$, $\Sigma^{*+,0}$, p , n , Σ^0 , Λ , we have

$$\begin{aligned} |\Delta^{++}; \uparrow\downarrow\uparrow\rangle &= u(1)u(2)u(3)|\uparrow\downarrow\uparrow\rangle, \\ |\Delta^-; \uparrow\downarrow\uparrow\rangle &= d(1)d(2)d(3)|\uparrow\downarrow\uparrow\rangle, \\ |\Delta^+; \uparrow\downarrow\uparrow\rangle &= \frac{1}{\sqrt{3}}[u(1)u(2)d(3) + u(1)d(2)u(3) \\ &\quad + d(1)u(2)u(3)]|\uparrow\downarrow\uparrow\rangle, \\ |\Delta^0; \uparrow\downarrow\uparrow\rangle &= (|\Delta^+; \uparrow\downarrow\uparrow\rangle \text{ with } u \leftrightarrow d), \\ |\Sigma^{*+}; \uparrow\downarrow\uparrow\rangle &= (|\Delta^+; \uparrow\downarrow\uparrow\rangle \text{ with } d \leftrightarrow s), \\ |\Sigma^{*0}; \uparrow\downarrow\uparrow\rangle &= \frac{1}{\sqrt{6}}[u(1)d(2)s(3) + \text{permutation}]|\uparrow\downarrow\uparrow\rangle, \end{aligned}$$

$$\begin{aligned}
|p; \uparrow\downarrow\uparrow\rangle &= \left[\frac{d(1)u(3) + u(1)d(3)}{\sqrt{6}} u(2) \right. \\
&\quad \left. - \sqrt{\frac{2}{3}} u(1)d(2)u(3) \right] |\uparrow\downarrow\uparrow\rangle, \\
|n; \uparrow\downarrow\uparrow\rangle &= (-|p; \uparrow\downarrow\uparrow\rangle \text{ with } u \leftrightarrow d), \\
|\Sigma^0; \uparrow\downarrow\uparrow\rangle &= \left[-\frac{u(1)d(3) + d(1)u(3)}{\sqrt{3}} s(2) \right. \\
&\quad \left. + \frac{u(2)d(3) + d(2)u(3)}{2\sqrt{3}} s(1) \right. \\
&\quad \left. + \frac{u(1)d(2) + d(1)u(2)}{2\sqrt{3}} s(3) \right] |\uparrow\downarrow\uparrow\rangle, \\
|\Lambda; \uparrow\downarrow\uparrow\rangle &= \left[\frac{d(2)u(3) - u(2)d(3)}{2} s(1) \right. \\
&\quad \left. + \frac{u(1)d(2) - d(1)u(2)}{2} s(3) \right] |\uparrow\downarrow\uparrow\rangle, \quad (\text{A2})
\end{aligned}$$

for the corresponding $|\mathbf{B}; \uparrow\downarrow\uparrow\rangle$ parts, while the 12- and 23-symmetric parts can be obtained by permutation. To be consistent with Eq. (14), our Λ state has an overall negative sign with respect to that of Ref. [36].

Following Ref. [36] and using the helicity argument in Sec. IV, asymptotically we have

$$\begin{aligned}
\langle \mathbf{B}(p_1) | \mathcal{O} | \overline{B} \mathbf{B}'(p_2) \rangle &= \bar{u}(p_1) \left[\frac{1 - \gamma_5}{2} F(t) \right] u(p_2), \\
F(t) &= \sum_{i=T, P_L, P_R} e_i (\mathbf{B}' - B - \mathbf{B}) F_i(t), \quad (\text{A3})
\end{aligned}$$

where \mathcal{O} are the operators in H_{eff} . For simplicity, we illustrate with the space-like case. Note that the above equation is obtained in the large $t (= (p_1 - p_2)^2)$ limit, where we may take a large m_B limit or view the B meson as a virtual particle with a large momentum. Quark mass dependent terms behave like $m_q/\sqrt{|t|}$ and are neglected. As shown in Fig. 2(a), the tree operator $(\bar{u}b)_{V-A}(\bar{d}u)_{V-A}$ can generate a $\mathbf{B}'(q'_R u_L q_R) - \overline{B}(\bar{q}'_L b) - \mathbf{B}(u_L d_L q_R)$ coupling. The corresponding coefficient $e_T(\mathbf{B}' - \overline{B} - \mathbf{B})$ is given by

$$\begin{aligned}
e_T(\mathbf{B}' - \overline{B} - \mathbf{B}) &= \langle \mathbf{B}; \downarrow\downarrow\uparrow | Q[q'_R(1) \rightarrow u_L(1); u_L(2) \rightarrow d_L(2)] | \mathbf{B}'; \uparrow\downarrow\uparrow \rangle \\
&\quad + \langle \mathbf{B}; \uparrow\downarrow\uparrow | Q[q'_R(3) \rightarrow u_L(3); u_L(2) \rightarrow d_L(2)] | \mathbf{B}'; \uparrow\downarrow\uparrow \rangle, \quad (\text{A4})
\end{aligned}$$

where $Q[q'_R(1(3)) \rightarrow u_L(1, 3); u_L(2) \rightarrow d_L(2)]$ changes the $q'(1(3))|\uparrow\rangle \otimes u(2)|\downarrow\rangle$ part of $|\mathbf{B}'; \uparrow\downarrow\uparrow\rangle$ to the $u(1(3))|\downarrow\rangle \otimes d(2)|\downarrow\rangle$ part.

Similarly coefficients $e_{P_L, P_R}(\mathbf{B}' - \overline{B} - \mathbf{B})$ for the $\mathbf{B}'(q'_R q_L q''_R) - \overline{B}(\bar{q}'_L b) - \mathbf{B}(d_L q_L q''_R)$ and $\mathbf{B}'(q'_R q_R q''_L) - \overline{B}(\bar{q}'_L b) - \mathbf{B}(d_L q_R q''_L)$ couplings governed respectively by

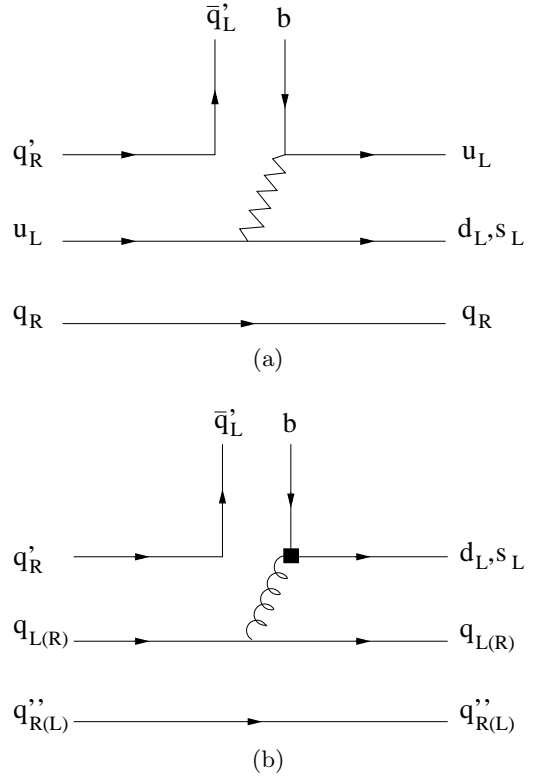


FIG. 2: (a) Tree and (b) penguin $\mathbf{B}' - \overline{B} - \mathbf{B}$ diagrams in the asymptotic limit.

TABLE IX: The coefficients $e_{T,P}(\mathbf{B}' - \overline{B} - \mathbf{B})$ for various modes obtained from Eqs. (A4, A5).

$\mathbf{B}' - \overline{B} - \mathbf{B}$	e_T	e_P	$\mathbf{B}' - \overline{B} - \mathbf{B}$	e_T	e_P
$\Sigma^{*0} - \overline{B}^0 - \Sigma^{*0}$	$\frac{1}{3}$	$\frac{2}{3}$	$\Delta^0 - B^- - \Delta^-$	0	$\frac{2}{\sqrt{3}}$
$\Delta^+ - B^- - \Delta^0$	$\frac{2}{3}$	$\frac{4}{3}$	$\Delta^+ - B^- - \Sigma^{*0}$	$\frac{\sqrt{2}}{3}$	$\frac{2\sqrt{2}}{3}$
$\Delta^{++} - B^- - p$	$\sqrt{\frac{2}{3}}$	$\sqrt{\frac{2}{3}}$	$\Sigma^{*0} - \overline{B}^0 - \Lambda$	0	$-\frac{1}{\sqrt{6}}$
$\Delta^+ - \overline{B}^0 - p$	$\frac{\sqrt{2}}{3}$	$\frac{\sqrt{2}}{3}$	$\Delta^+ - B^- - n$	$-\frac{\sqrt{2}}{3}$	$\frac{\sqrt{2}}{3}$
$\Sigma^{*+} - \overline{B}_s^0 - p$	$\frac{\sqrt{2}}{3}$	$\frac{\sqrt{2}}{3}$	$\Delta^+ - B^- - \Sigma^0$	$\frac{1}{3}$	$\frac{2}{3}$
$p - B^- - \Delta^0$	$\frac{\sqrt{2}}{3}$	$-\frac{\sqrt{2}}{3}$	$p - \overline{B}^0 - \Delta^+$	$\frac{\sqrt{2}}{3}$	$\frac{\sqrt{2}}{3}$
$n - B^- - \Delta^-$	0	$-\sqrt{\frac{2}{3}}$	$\Lambda - \overline{B}^0 - \Sigma^{*0}$	$-\frac{1}{\sqrt{6}}$	$-\frac{1}{\sqrt{6}}$
$p - B^- - \Sigma^{*0}$	$\frac{1}{3}$	$-\frac{1}{3}$	$n - \overline{B}^0 - \Sigma^{*0}$	$\frac{2}{3}$	$\frac{1}{3}$
$p - \overline{B}^0 - p$	$\frac{1}{3}$	$\frac{1}{3}$	$p - B^- - n$	$-\frac{1}{3}$	$-\frac{5}{3}$
$n - \overline{B}^0 - n$	$-\frac{2}{3}$	$-\frac{4}{3}$	$\Lambda - \overline{B}^0 - \Sigma^0$	$-\frac{1}{\sqrt{3}}$	$\frac{1}{\sqrt{3}}$
$\Sigma^0 - \overline{B}^0 - \Sigma^0$	$-\frac{1}{3}$	$-\frac{2}{3}$	$\Sigma^0 - \overline{B}^0 - \Lambda$	0	$\frac{\sqrt{3}}{2}$
$\Lambda - \overline{B}^0 - \Lambda$	0	0	$n - \overline{B}^0 - \Lambda$	$\sqrt{\frac{2}{3}}$	$\sqrt{\frac{3}{2}}$
$p - B^- - \Sigma^0$	$\frac{1}{\sqrt{18}}$	$-\frac{1}{3\sqrt{2}}$	$p - B^- - \Lambda$	$\frac{1}{3\sqrt{2}}$	$\sqrt{\frac{3}{2}}$

the penguin operators $(\bar{d}b)_{V-A}(\bar{q}q)_{V\mp A}$ are given by

$$\begin{aligned} e_{P_L}(\mathbf{B}' - \bar{\mathbf{B}} - \mathbf{B}) \\ = \langle \mathbf{B}; \downarrow\downarrow\uparrow | Q[q'_R(1) \rightarrow d_L(1); q_L(2) \rightarrow q_L(2)] | \mathbf{B}'; \uparrow\downarrow\uparrow \rangle \\ + \langle \mathbf{B}; \uparrow\downarrow\downarrow | Q[q'_R(3) \rightarrow d_L(3); q_L(2) \rightarrow q_L(2)] | \mathbf{B}'; \uparrow\downarrow\uparrow \rangle, \\ e_P(\mathbf{B}' - \bar{\mathbf{B}} - \mathbf{B}) \equiv e_{P_L}(\mathbf{B}' - \bar{\mathbf{B}} - \mathbf{B}) \\ = e_{P_R}(\mathbf{B}' - \bar{\mathbf{B}} - \mathbf{B}). \end{aligned} \quad (A5)$$

The corresponding diagram is shown in Fig. 2(b). Note that that e_{P_L} is similar to e_T with the $q'_R(1, 3) \rightarrow u_L(1, 3)$ and $u_L(2) \rightarrow d_L(2)$ operations replaced by the $q'_R(1, 3) \rightarrow d_L(1, 3)$ and $q_L(2) \rightarrow q_L(2)$ operations, respectively. The equality of e_{P_R} and e_{P_L} can be understood by interchanging $q \leftrightarrow q''$ in $\mathbf{B}'(q'_R q_L q''_R) - \bar{\mathbf{B}}(\bar{q}'_L b) - \mathbf{B}(d_L q_L q''_R)$ and $\mathbf{B}'(q'_R q_R q''_L) - \bar{\mathbf{B}}(\bar{q}'_L b) - \mathbf{B}(d_L q_R q''_L)$. The coefficients for the $|\Delta S| = 1$ case can be obtained by the suitable

replacement of $d_L \rightarrow s_L$ in the \mathbf{B} content in Eqs. (A4, A5).

As shown Table IX the octet-octet, octet-decuplet and decuplet-decuplet systems are related asymptotically [36]. With

$$\begin{aligned} T^{(\prime)} &\propto \frac{1}{3} V_{ub} V_{ud(s)}^* F_T \bar{u}_R v_L, \\ P^{(\prime)} &\propto \frac{1}{3} V_{tb} V_{td(s)}^* (F_{P_L} + \kappa^{(\prime)} F_{P_R}) \bar{u}_R v_L, \end{aligned} \quad (A6)$$

where $\kappa^{(\prime)}$ as the ratio of the corresponding Wilson coefficients of the $(\bar{d}b)_{V-A}(\bar{q}q)_{V\pm A}$ $((\bar{d}s)_{V-A}(\bar{q}q)_{V\pm A})$ operators, we obtain the asymptotic relations, Eqs. (32–37), by comparing Table IX with the corresponding amplitudes shown in Tables I–V.

[1] S. Anderson *et al.* [CLEO Collaboration], Phys. Rev. Lett. **86**, 2732 (2001).

[2] K. Abe *et al.* [Belle Collaboration], Phys. Rev. Lett. **89**, 151802 (2002).

[3] K. Abe *et al.* [Belle Collaboration], Phys. Rev. Lett. **88**, 181803 (2002).

[4] M.Z. Wang [Belle Collaboration], arXiv:hep-ex/0305060.

[5] M. Z. Wang *et al.* [Belle Collaboration], Phys. Rev. Lett. **90**, 201802 (2003).

[6] N. Gabyshev and H. Kichimi *et al.* [Belle Collaboration], hep-ex/0212052.

[7] K. Abe *et al.* [Belle Collaboration], Phys. Rev. D **65**, 091103 (2002).

[8] K. Hagiwara *et al.* [Particle Data Group Collaboration], Phys. Rev. D **66**, 010001 (2002).

[9] W.S. Hou and A. Soni, Phys. Rev. Lett. **86**, 4247 (2001).

[10] C.K. Chua, W.S. Hou and S.Y. Tsai, Phys. Rev. D **65**, 034003 (2002).

[11] C.K. Chua, W.S. Hou and S.Y. Tsai, Phys. Lett. B **528**, 233 (2002).

[12] H.Y. Cheng and K.C. Yang, Phys. Rev. D **66**, 014020 (2002).

[13] H.Y. Cheng and K.C. Yang, Phys. Rev. D **66**, 094009 (2002).

[14] C.K. Chua, W.S. Hou and S.Y. Tsai, Phys. Rev. D **66**, 054004 (2002).

[15] C. K. Chua and W. S. Hou, arXiv:hep-ph/0211240, to appear in Eur. Phys. J. C.

[16] J. L. Rosner, arXiv:hep-ph/0303079.

[17] S. Arunagiri and C. Q. Geng, arXiv:hep-ph/0305268.

[18] N. G. Deshpande, J. Trampetic and A. Soni, Mod. Phys. Lett. **3A**, 749 (1988).

[19] M. Jarfi, O. Lazrak, A. Le Yaouanc, L. Oliver, O. Pene and J. C. Raynal, Phys. Rev. D **43**, 1599 (1991).

[20] H. Y. Cheng and K. C. Yang, Phys. Rev. D **65**, 054028 (2002) [Erratum-ibid. D **65**, 099901 (2002)].

[21] V. L. Chernyak and I. R. Zhitnitsky, Nucl. Phys. B **345**, 137 (1990).

[22] P. Ball and H. G. Dosch, Z. Phys. C **51**, 445 (1991).

[23] C. H. Chang and W. S. Hou, Eur. Phys. J. C **23**, 691 (2002).

[24] M. Gronau and J. L. Rosner, Phys. Rev. D **37**, 688 (1988).

[25] M. J. Savage and M. B. Wise, Nucl. Phys. B **326**, 15 (1989).

[26] X. G. He, B. H. McKellar and D. d. Wu, Phys. Rev. D **41**, 2141 (1990).

[27] S. M. Sheikholeslami and M. P. Khanna, Phys. Rev. D **44**, 770 (1991).

[28] S. M. Sheikholeslami, G. K. Sidana and M. P. Khanna, Int. J. Mod. Phys. A **7**, 1111 (1992).

[29] Z. Luo and J. L. Rosner, arXiv:hep-ph/0302110.

[30] D. Zeppenfeld, Z. Phys. C **8**, 77 (1981).

[31] L. L. Chau and H. Y. Cheng, Phys. Rev. D **36**, 137 (1987).

[32] L. L. Chau, H. Y. Cheng, W. K. Sze, H. Yao and B. Tseng, Phys. Rev. D **43**, 2176 (1991) [Erratum-ibid. D **58**, 019902 (1998)].

[33] M. Gronau, O. F. Hernandez, D. London and J. L. Rosner, Phys. Rev. D **50**, 4529 (1994).

[34] M. Gronau, O. F. Hernandez, D. London and J. L. Rosner, Phys. Rev. D **52**, 6374 (1995).

[35] H. Y. Cheng, Phys. Rev. D **65**, 094012 (2002); C. W. Chiang and J. L. Rosner, Phys. Rev. D **67**, 074013 (2003).

[36] S.J. Brodsky, G.P. Lepage and S.A. Zaidi, Phys. Rev. D **23**, 1152 (1981).

[37] G.P. Lepage and S.J. Brodsky, Phys. Rev. Lett. **43**, 545 (1979) [Erratum-ibid. **43**, 1625 (1979)].

[38] M. J. Savage and M. B. Wise, Phys. Rev. D **39**, 3346 (1989) [Erratum-ibid. D **40**, 3127 (1989)].

[39] T. D. Lee, Contemp. Concepts Phys. **1**, 1 (1981); H. Georgi, *Weak Interactions And Modern Particle Theory*, Benjamin/Cummings, 1984.

[40] T. Moroi, arXiv:hep-ph/9503210; S. Deser, V. Pascalutsa and A. Waldron, Phys. Rev. D **62**, 105031 (2000).

[41] B. Aubert *et al.* [BABAR Collaboration], arXiv: hep-ex/0303028; A. Bornheim *et al.* [CLEO Collaboration], arXiv: hep-ex/0302026; T. Tomura, [Belle Collaboration], arXiv:hep-ex/0305036.